1966

An investigation of the secondary flow phenomena in a cascade of high-deflection axial-flow impulse turbine blades

Bown, Rodney Loren

Monterey, California. U.S. Naval Postgraduate School

AN INVESTIGATION OF THE SECONDARY FLOW PHENOMENA IN A CASCADE OF HIGH-DEFLECTION AXIAL-FLOW IMPULSE TURBINE BLADES

RODNEY LOREN BOWN

AN INVESTIGATION OF THE SECONDARY FLOW PHENOMENA IN A CASCADE OF HIGH-DEFLECTION AXIAL-FLOW IMPULSE TURBINE BLADES

by

Rodney Loren Bown
Captain, United States Marine Corps
B.S., University of Washington, 1958

Submitted in partial fulfillment
of the requirements
for the degree of

MASTER OF SCIENCE IN AERONAUTICAL ENGINEERING

from the

UNITED STATES NAVAL POSTGRADUATE SCHOOL
December 1966

ABSTRACT

Cascade tests were performed on models of the rotor blades of a high-deflection, axial-flow impulse turbine to determine the secondary flow losses. The tests were performed at the Rectilinear Cascade Test Facility of the Turbo-Propulsion Laboratories of the Department of Aeronautics, Naval Postgraduate School. The results were compared with the predicted losses from various formulas that have been proposed in the technical literature. The comparison showed that most formulas predict a secondary loss that is about ten times as high as that determined in the present tests. Photographs were obtained of the boundary layer traces by the use of lamp black coating. These photographs show the effects of secondary flows on the performance of a cascade.

AN INVESTIGATION OF THE SECONDARY FLOW PHENOMENA IN A CASCADE OF HIGH-DEFLECTION AXIAL-FLOW IMPULSE TURBINE BLADES

by

Rodney Loren Bown
Captain, United States Marine Corps
B.S., University of Washington, 1958

Submitted in partial fulfillment
of the requirements
for the degree of

MASTER OF SCIENCE IN AERONAUTICAL ENGINEERING

from the

UNITED STATES NAVAL POSTGRADUATE SCHOOL
December 1966

ABSTRACT

Cascade tests were performed on models of the rotor blades of a high-deflection, axial-flow impulse turbine to determine the secondary flow losses. The tests were performed at the Rectilinear Cascade Test Facility of the Turbo-Propulsion Laboratories of the Department of Aeronautics, Naval Postgraduate School. The results were compared with the predicted losses from various formulas that have been proposed in the technical literature. The comparison showed that most formulas predict a secondary loss that is about ten times as high as that determined in the present tests. Photographs were obtained of the boundary layer traces by the use of lamp black coating. These photographs show the effects of secondary flows on the performance of a cascade.

TABLE OF CONTENTS

LIST OF TABLES

LIST OF ILLUSTRATIONS

TABLE OF SYMBOLS

a	minimum distance between blades, in.
c	chord of test blade, in.
C_D	drag coefficient, dimensionless
C_L	lift coefficient, dimensionless
D	drag force, lb./ft.
D_h	hydraulic diameter, in.
g	gravitational constant, ft./sec.^{2}
h	test blade height, in.
K_{te}	constant for exit angle prediction, dimensionless
L	lift force, lb./ft.
M	Mach number, dimensionless
P	absolute static pressure, lb./ft.^{2}
Pt	absolute total pressure, lb./ft.^{2}
Rey	Reynolds number, dimensionless
s	blade spacing, in.
T	temperature, ^oR
t_e	blade thickness in the discharge plane, in.
t	minimum blade thickness perpendicular to exit velocity, in.
V	fluid velocity, ft./sec.
y	distance along blade height, in.
Y	pressure loss coefficient, dimensionless
α	flow angle
γ	ratio of specific heats, dimensionless
ζ	loss coefficient, dimensionless
λ	constant for secondary flow, dimensionless
μ	viscosity, lb./ft.-sec.

ρ	mass density, lb.-sec^2/ft.^{4}
σ	blade row solidity, $\frac{c}{s}$, dimensionless
ϕ	velocity coefficient, dimensionless

Subscripts

0	station 0, far ahead of the cascade
2	station 2, downstream measuring plane
th	theoretical
∞	Vectorial mean of conditions at station 0 and 3
s	secondary
2D	two-dimensional

1. Introduction

The necessity to produce large amounts of power in a turbine stage requires the use of low reaction blades with large gas deflections. The Rectilinear Cascade and the Transonic Turbine Test Rig located at the Turbo-Propulsion Laboratory of the Department of Aeronautics, Naval Postgraduate School, are being used to investigate the flow in such turbine states. Previous tests were conducted in the Rectilinear Cascade Test Facility to determine the profile losses of a turbine stage. [7] The cascade data were compared with the results obtained with an actual turbine in a rotating test rig.

For the present study a rectilinear cascade was used to investigate the secondary flow phenomena in a rotor blade cascade. The rotor blades were tested at two different inlet angles. The tests were conducted at a Mach number of approximately 0.20 and a Reynolds number of about 1.0×10^6. The results are compared with published results in the technical literature. Photographs were made of the boundary layer flow patterns by using lamp black coating on the walls and the blades.

2. Installation

The Rectilinear Cascade Test Facility is an open cycle wind tunnel used to investigate the flow in rectilinear cascades of axial turbomachines. The Cascade Laboratory and associated equipment are described by Rose and Guttormson. [12] The plenum chamber was modified by Bartocci. [8] The present installation of the cascade is described by Bartocci. [7]

The rotor profile geometry is shown in Fig. 1. Of note is the fact that it is composed solely of straight lines and circular arcs, that the leading and trailing edges are not rounded, and that the blade

shape is designed for a large flow deflection, namely 132 degrees. The rotor blade models have a chord of 6.757 inches and a blade spacing of four inches. The solidity is 1.69 and the span is ten inches. The span to chord ratio is 1.48. The stagger angle is -4.50 degrees. The blades are nine times scale models of the blades at the mean radius of a turbine rotor that can be installed in the Transonic Turbine Test Rig at the Turbo-Propulsion Laboratory of the Naval Postgraduate School. The cascade geometry is shown in Fig. 2. The inlet and exit angles are shown at the measuring planes.

The inlet and exit flow angles, total pressures, and dynamic pressures were measured at 0.05 inch increments across the middle two blades of the cascade. The Automatic Data Logging System was used to obtain the data for the first five tests. A mechanical failure occurred during the sixth test. The system then required recalibration. During this procedure several electrical failures occurred. It was then decided to complete the remaining tests by using water-filled manometer tubes. One test run could be completed in one and one-half hours with the Automatic Data Logging System. Four to five hours were required to complete a test run when the manometer tubes were read directly.

Pressure and flow measurements were made by using two United Sensor and Control Corporation YC-120 flow probes. The calibration data for the probes were obtained from the curves provided by the vendor. The probes were subject to considerable error when used close to a wall. An immersion calibration was performed on both probes. The probes had essentially an equal error. An immersion correction was not used since the loss coefficient depends on the ratio of dynamic pressures ahead of

and after the cascade, and the correction cancels in the computation. During the immersion calibration the vendor's calibration curves were checked and found to be sufficiently accurate.

The probe after the cascade vibrated considerably when it was cantilevered in excess of eight inches. The lower probe remained quite steady throughout its spanwise travel. This demonstrated that the probes were structurally stiff enough but that the flow downstream of the blade row caused the upper probe to vibrate. An airfoil was fitted to the upper probe in an attempt to decrease the vibration, but this change was unsuccessful. For this reason the upstream data for y = 9.0 and 9.25 inches should be used in a cautious manner.

For the first series of tests the inlet side walls were set at 66.0 degrees. The average inlet flow angle in the center of the cascade was 67.2 degrees. The flow does not follow the inlet walls exactly but seeks a path of least resistance. Experience has shown that the air inlet angle to the blade row was approximately one degree greater than the inlet wall geometry. The second series of test was conducted with the walls at 62.0 degrees. The average inlet flow angle in the center of the cascade was 62.7 degrees. The gap between the tip of the blades and the adjacent wall was blocked by rubber pieces glued to the profile to eliminate tip clearance flows.

The inlet angles were chosen to correspond to previous tests conducted with the blades. The minimum loss coefficient determined by Bartocci occurred at an inlet angle of 66.2 degrees. [7] The design inlet angle is 62.0 degrees.

3. Definition of Parameters

The Reynolds number is defined as

$$Rey = \frac{\rho_3 V_3 c}{\mu} \tag{1}$$

The Mach number is defined as

$$M = \frac{V_o}{\sqrt{\gamma g R T_o}} \tag{2}$$

The velocity coefficient for the flow through a cascade is defined as

$$\phi = \frac{V}{V_{th}} \tag{3}$$

The loss coefficient for the cascade is defined as

$$\zeta' = 1 - \left(\frac{V_3}{V_{3th}}\right)^2 \tag{4}$$

This loss coefficient corresponds to the cascade efficiency as given by Vavra.[1]

Two other loss coefficients are used to correlate the cascade tests to other published results. These are the stagnation pressure loss coefficients used by Ainley and Mathieson, and the enthalpy loss coefficient which is related to the actual exit velocity. [4] The stagnation pressure loss coefficient is defined as

$$Y = \frac{P_{to} - P_{t3}}{P_{t3} - P_3} \tag{5}$$

The enthalpy loss coefficient is defined as

$$\zeta = \frac{V_{3th}^2 - V_3^2}{V_3^2} = \frac{V_{3th}^2}{V_3^2} - 1 \tag{6}$$

The enthalpy loss coefficient was used by Bartocci. [7] The loss

[1] Vavra, M.H., Aerothermodynamics and Flows in Turbomachines (New York: John Wiley and Sons, Inc., 1960) pp. 83.

coefficients are related by

$$\zeta = \frac{\zeta'}{1-\zeta'} \tag{7}$$

The lift and drag coefficients are defined as

$$C_{L_\infty} = \frac{L}{\frac{1}{2}\rho V_\infty^2 c} \tag{8}$$

and

$$C_{D_\infty} = \frac{D}{\frac{1}{2}\rho V_\infty^2 c} \tag{9}$$

where c is the blade chord and

$$\rho = \frac{1}{2}(\rho_0 + \rho_3) \tag{10}$$

V_∞ is the magnitude of the mean vectorial velocity of V_0 and V_3.

L and D are the forces per unit blade height acting on the blade perpendicular and parallel to V_∞. L and D are components of the resultant force acting on the blade which is computed by the momentum equation.

4. Results and Discussion

The test results are presented in Tables I and II. The experimental data, computer results, and graphs of the total, dynamic, and static pressures are filed in a separate cover at the Cascade Laboratory. In Fig. 3 the loss coefficient ζ' is plotted versus the blade height for both series of tests. The exit angles are plotted in a similar fashion on Fig. 4. The enthalpy loss coefficient ζ is plotted on Fig. 5, and the stagnation pressure loss coefficient Y is plotted on Fig. 6.

The loss coefficients include the mixing losses since the upper measuring plane was approximately 29 inches aft of blades in the

direction of the discharge flow. The loss coefficient on the centerline of the cascade for an inlet flow angle of 66 degrees was essentially the same as previously determined by Bartocci. [7] This demonstrated that the Automatic Data Recording Equipment functioned correctly. The spanwise distribution of the loss coefficient indicated peak losses at the one-quarter span locations from the walls.

The loss coefficient distribution shows the effect of the secondary flows in the blade channels. Secondary flows occur when actual flows with boundary layers are turned in a channel. The result is the formation of the two trailing vortices shown in Fig. 7, which is a simplified reproduction from Vavra.[2] The trailing vortices cause a loss in addition to the profile and mixing losses. Fig. 8 shows an idealized three-dimensional flow through a row of blades as published by Ainley and Mathieson.[3] The spanwise loss coefficient distributions of Fig. 3 and Fig. 8 are qualitatively very similar. Fig. 3 does not show a uniform mid-span loss since the tested turbine blades have an aspect ratio of only 1.48.

Secondary flow theory predicts that the flow deflections will be greater at the end walls of the cascade than at the mid-span location. The exit angles shown in Fig. 4 confirm this prediction. The slightly smaller exit angles at y/h = 0.3 and y/h = 0.7 correspond to the decreased deflection of the flow by the secondary flow vortices that occur at points A and B in Fig. 7.

In Appendix A are calculated the exit flow angles by three differ-

[2]Ibid, pp. 376.

[3]Ainley, D.G. and Mathieson, G.C.R., An Examination of the Flow and Pressure Losses in Blade Rows of Axial Flow Turbines (A.R.C. R and M 2891) Fig. 15a, pp. 31.

ent formulas. The predicted exit angles are 0.8 to 1.9 degrees less than the experimental centerline exit angles.

The local loss coefficient ζ' of the cascade was plotted on Fig. 9 versus the dimensionless distance y/c where c is the chord. Also shown on Fig. 9 are two curves for an impulse rotor blade from Holliger.[4] The loss coefficient used by Holliger is defined as

$$\bar{\zeta} = \frac{P_{t_{3th}} - P_{t_3}}{P_{t_{3th}} - P_3} \tag{11}$$

where Pt_{3th} is the total pressure outside the wake. The index 3 refers to conditions after the cascade. The loss coefficient as defined by Holliger and the coefficient ζ' used in this paper are essentially the same, but Fig. 9 is intended for qualitative comparison only. The two tests by Holliger were conducted at two different aspect ratios. The curve for an aspect ratio of 3.48 illustrates a substantial two-dimensional region in the mid span area. The other curve for an aspect ratio of 0.619 shows that the zones of disturbance on the two walls have interacted in the center of the cascade. The curves on Fig. 9 show that the experimental loss coefficient ζ' and the loss coefficient measured by Holliger have maximum values at about the same relative wall clearance.

The turbine cascade results obtained by this writer demonstrate that the centerline loss coefficient is most likely free from secondary flow loss. The disturbance zone is in the same relative location from the wall as was found by Holliger. It was not possible to obtain accurate test data closer to the wall than shown in Fig. 9, therefore, the

[4]Holliger, K., Further Developments of Steam Turbine Blading (Escher Wyss News Vol. 33, 1960) pp. 79.

loss coefficients at the wall could not be compared.

Curves for reaction blades similar to the curves of Fig. 9 have been published by New. [11] One set of the curves are reproduced in Fig. 10. Efficiency rather than the loss coefficient is plotted. The efficiency as defined by New is compatible with the loss coefficient ζ' and the loss coefficient used by Holliger. An aspect ratio of 2.3 is required in the cascade used by New to obtain a two-dimensional flow in the center of the cascade whereas an aspect ratio of 1.48 is sufficient in the turbine cascade used by this writer. The difference in required aspect ratios can be partially explained by the comparative sizes of the cascades. The cascade used by New was smaller than the Turbine Cascade at the United States Naval Postgraduate School. The blades tested by New had a chord length equal to 1.70 inches compared to a chord length equal to 6.757 inches for the blade used by this writer. Assuming a similar boundary layer growth in both cascades the boundary layer in the smaller cascade would be relatively larger with respect to the span length than the boundary layer in the larger cascade. The secondary flow caused by the boundary layer would affect a larger portion of the span in the smaller cascade thereby requiring a larger aspect ratio for a two-dimensional flow region.

The two-dimensional secondary loss coefficient is considered to be the excess over the loss coefficient at the mid-span.

$$\zeta_s' = \zeta_{local}' - \zeta_{20}' \qquad (12)$$

The two-dimensional secondary loss coefficient shown on Fig. 3 was approximately equal to the profile loss and mixing loss coefficient at the one-quarter span locations from the wall. The profile and mixing

loss coefficient was assumed equal to 0.65 along the entire span for both inlet angles. The average total loss coefficient was determined by integrating the local loss coefficient over the blade span. These average total loss coefficients were found to be 0.095 for 66 degrees and 0.085 for 62 degrees side wall angles respectively. The average secondary loss coefficients were then 0.030 and 0.020 for the two side wall angles. The higher secondary loss coefficient for the larger deflection reflects the effect of the turning angle upon the secondary flow. The three overall loss coefficients, ζ', ζ, and Y, are shown in Table III.

Markov presents a characteristic spanwise change in loss coefficient for a rotor blade cascade that is very similar to Fig. 3 and is shown in Fig. 11.[5] The rotor blade profile consists of circular arcs and straight lines and is shown in Fig. 11. The design flow deflection is 124 degrees. The profile and secondary loss coefficient agree very well with the results found by this experimenter. The profile loss coefficient obtained by Markov was 0.062 and the overall loss coefficient was approximately 0.098.

Several methods for predicting the secondary flow loss coefficient are presented in Appendix B. The formula by Markov gives secondary loss coefficients that agree well with the experimental loss coefficients. For 62 degrees side wall angle the predicted secondary loss coefficient was 0.0206 compared to the experimental secondary loss coefficient of 0.020. The predicted loss coefficient for 66 degrees side wall angle was 0.0262 compared with the experimental loss coefficient of 0.030. Several authors have stated that the secondary loss coefficients pre-

[5]Markov, N.M., Calculation of the Aerodynamic Characteristics of Turbine Blading (New Jersey: Associated Technical Services, 1958) pp. 26.

dicted by Markov are too small, a condition which has not been found in the present case. Markov's formula appears to predict an accurate secondary flow loss coefficient for a high deflection turbine cascade.

The other formulas presented in Appendix B predict secondary flow loss coefficients that are one magnitude higher. If the actual turbine rotor is considered, these higher loss coefficients seem to be probable. The loss coefficients for the actual rotor were determined by Eckert. [9] The loss coefficients varied from 0.35 to over 0.50. Therefore, one can assume that the secondary loss coefficient in Eckert's case would be of the order 0.20 to 0.30.

Soderberg has attempted to correlate loss coefficients to a standard Reynolds number and aspect ratio.[6] The computations are shown in Appendix B. Soderberg's formula predicts an enthalpy loss coefficient ζ equal to 0.12 for the flow deflection of run 100 of Table I with the side walls at 66 degrees and a loss equal to 0.115 for the deflection of run 111 with the side walls at 62 degrees. The corresponding experimental values for ζ were 0.106 and 0.095. The correlation is limited to moderate deflection angles and blade thickness, hence, substantial extrapolation was required to obtain Soderberg's loss coefficients. The loss coefficients compare favorably in spite of the limitations of the correlation. Ainley and Mathieson predict a secondary loss coefficient that is also high.[7] For the conditions of the inlet side walls at 62 degrees the calculated secondary loss coefficient is 0.13 compared with value of 0.023 measured by this writer.

[6]Horlock, J.H., Axial Flow Turbines (London: Butterworth and Company, 1966) pp. 86-88.

[7]Ainley, op. cit., pp. 17.

The loss coefficients are dependent upon the Reynolds number. Horlock in referring to other experimenters suggests that the loss coefficient is proportional to the one-fifth power of the Reynolds number above a critical value of $10^{5.8}$ The Reynolds number is based on the hydraulic diameter, D_h:

$$D_h = \frac{2 h s \cos\alpha_3}{s \cos\alpha_3 + h} \tag{13}$$

The hydraulic diameter of the tested turbine cascade for an exit angle of 71.0 degrees is 2.30 inches. This compares with the chord length of 6.757 inches used by this writer as the characteristic length. The Reynolds numbers for the cascade based on D_h would be 34 percent of those listed in Tables I and II. The loss coefficients of Tables I and II can be correlated to those of Horlock or Ainley and Mathieson if they are compared at the Reynolds number based on the hydraulic diameter.

A low reaction blade does not have a very favorable pressure gradient and comparatively thick boundary layers are unavoidable. A typical outlet velocity distribution from a low reaction turbine stage is shown in Fig. 12 which has been reproduced from Ainley and Mathieson.[9] A major thickening of the boundary layer has occurred at the blade root; at the tip the flow is accelerated through the radial tip clearance. A major portion of the secondary loss appears to occur in the vicinity of the blade root where the local flow accelerations through the row are smallest. With high reaction turbines the velocity distribution is more uniform and the secondary losses should be smaller.

The average acceleration in the turbine cascade tested by this

[8]Horlock, op. cit., pp. 102.

[9]Ainley, op. cit., Fig. 19, pp. 33.

writer was from 240 to 330 feet per second. The accelerated flow in the tested turbine cascade provides a favorable pressure gradient that should cause a lower secondary loss compared with the secondary loss for an impulse turbine cascade. Therefore, the secondary loss coefficient measured by this writer should be smaller compared with the secondary loss coefficient that is predicted in most of the technical literature for an impulse turbine cascade. For this reason it seems beneficial to provide for a certain amount of flow acceleration in a blade row, particularly for those with large flow deflections.

The boundary layer flow within the blade row was investigated by the use of lamp black coatings. Some of the resulting pictures are shown in Figs. 13 to 17. The convex sides of the two middle blades are shown in Figs. 13, 14 and 15 with the leading edge towards the right of the figures. The flow in the boundary layer starts away from the ends at the point where the blade curvature begins. This is at point A in Fig. 1. The flow in the mid-span portion of the blades appears to be very closely two-dimensional. Fig. 16 shows the concave side of the blades.

Fig. 17 shows the flow in the side wall boundary layer. The direction of the flow is from the high pressure concave side of one blade to the low pressure convex side of the adjacent blade. This flow pattern agrees well with what can be predicted from secondary flow theory (Fig. 7).

The computer program "CASCADE" was used to process the test data and to calculate the cascade parameters. The computer program is explained by Bartocci. [7] Three modifications were made by this writer. The input and output statements were changed to suit the particular needs

of the tests. One arithmetic statement was corrected and the loss coefficient was redefined to obtain the loss coefficient ζ'. The enthalpy loss coefficient ζ can be obtained from ζ' by Eq. (7).

5. Conclusions

The test results have demonstrated the effect and the magnitude of the losses, due to secondary flow in a cascade of turbine blades. The loss coefficient distribution along the blade height agrees well with the results published by Markov, Holliger, and New. The magnitude of the secondary loss coefficient agrees with the secondary loss coefficient predicted by Markov. Most other published formulas give secondary loss coefficients about ten times as large as the secondary loss coefficients measured by this writer.

The accelerated flow in the tested turbine cascade provides a favorable pressure gradient that tends to slow the growth of the boundary layer. The secondary flow caused by the formation of the boundary layer would then be smaller in the tested turbine cascade compared with an impulse turbine cascade without accelerated flow. Therefore, the formulas that predict secondary loss coefficients for an impulse turbine cascade would give a loss coefficient that is too large for the tested turbine cascade.

Although there exists a good qualitative understanding of secondary flow phenomena, the different available quantitative predictions of the secondary flow loss vary greatly in magnitude. The method of Markov appears to give the best prediction of the secondary losses for cascades of turbine blades.

6. Recommendations and Acknowledgements

The cascade facility is operating well except for the Automatic Data

Logging System. If the funds are not available for the acquisition of a faster and more accurate system, serious effort should be made to modify the present equipment to ensure satisfactory operation. The potential of the Cascade Test Rig can not be reached if about four hours are required to complete one experimental run, and if two additional hours are required to punch the computer data cards.

Several blade tests should be carried out in the near future. The effect of tip clearance flows should be determined and compared with the two-dimensional secondary flow results of this thesis. A blade similar to the present blade but with a rounded blunt leading edge should be tested. The blunt leading edge permits the incidence angle to vary without decreasing the blade performance. Such a blade can be used in turbines at low Mach numbers and varying incidence angle.

Flow visualization studies should be conducted with improved means of introducing smoke into the test section. The boundary layers on the walls and the blades should be investigated. If pressure taps were installed in a blade, the upper and lower surface pressure patterns could be determined to correlate secondary flow phenomena with boundary layer patterns.

The Cascade Test Rig has the provision for the removal of the side wall boundary layer upstream of the lower measureing plane. The effect of the side wall boundary layer on the secondary loss ahould be investigated by the use of a boundary layer removal system.

The writer wishes to express his appreciation to Mr. R.W. Savage for the patience, loyalty, skill, and assistance he provided during this investigation, and to the guidance provided by Dr. M. H. Vavra.

TABLE I

Test Results for Inlet Side Walls at 66 Degrees

y	Run No.	ζ'	ζ	Y	α_0	$\sim\alpha_0$	α_3	$\sim\alpha_3$
0.75	105	0.065	0.070	0.072	67.0	0.4	-77.8	0.6
1.00*	104	0.072	0.078	0.081	66.6	0.8	-76.1	0.7
2.00	110	0.120	0.136	0.143	67.6	0.8	-72.1	0.9
3.00*	101	0.118	0.133	0.138	66.9	0.5	-69.6	1.6
4.00	106	0.075	0.081	0.085	67.3	0.6	-70.9	0.6
5.00*	100	0.065	0.070	0.073	67.2	0.4	-70.8	0.8
6.00	107	0.079	0.086	0.090	67.1	0.4	-70.8	0.6
7.00*	102	0.138	0.160	0.167	66.9	0.5	-69.1	1.9
8.00	109	0.124	0.142	0.148	67.5	0.5	-71.2	1.1
9.00*	103	0.055	0.059	0.061	67.6	0.6	-75.1	1.3
9.25	108	0.038	0.042	0.042	67.8	0.3	-76.5	0.5

* Automatic Data Logging System

$\sim\alpha$ Maximum deviation of the angle

TABLE I (cont.)

Test Results for Inlet Side Walls at 66 Degrees

y	$\Delta\alpha$	C_{L_∞}	C_{D_∞}	Rey $\times 10^{-6}$	M	V_0	V_3
0.75	144.8	6.95	0.726	1.04	0.198	224.4	307.5
1.00	142.7	6.59	0.634	1.05	0.197	222.7	307.8
2.00	139.7	6.36	0.684	1.08	0.212	239.4	314.6
3.00	136.5	5.84	0.473	1.08	0.210	237.4	314.3
4.00	138.2	5.95	0.283	1.13	0.220	249.2	334.3
5.00	138.0	5.86	0.199	1.14	0.213	241.2	332.3
6.00	137.9	5.93	0.307	1.12	0.216	245.0	328.9
7.00	136.0	5.81	0.570	1.01	0.209	239.7	315.6
8.00	138.7	6.22	0.653	1.09	0.218	246.2	318.0
9.00	142.7	6.39	0.366	1.10	0.197	222.6	321.3
9.25	144.3	6.58	0.361	1.09	0.196	222.1	319.3

TABLE II

Test Results for Inlet Side Walls at 62 Degrees

y	Run No.	δ'	δ	Y	α_0	$\sim\alpha_0$	α_3	$\sim\alpha_3$
0.75	118	0.122	0.140	0.145	62.0	0.8	-77.3	0.4
1.00	117	0.094	0.103	0.107	62.0	0.9	-76.6	0.5
2.00	116	0.112	0.127	0.132	62.6	0.5	-70.4	0.6
3.00	112	0.083	0.091	0.094	62.7	0.5	-70.8	0.6
4.00	114	0.068	0.073	0.076	62.5	0.5	-71.9	0.2
5.00	111	0.065	0.070	0.072	62.8	0.6	-71.6	0.4
6.00	115	0.070	0.075	0.079	62.3	0.6	-72.0	0.4
7.00	113	0.085	0.094	0.097	62.6	0.5	-70.9	0.4
8.00	120	0.117	0.133	0.134	61.9	0.4	-70.2	1.0
9.00	119	0.070	0.075	0.079	63.0	0.2	-75.1	0.4
9.25	121	0.058	0.061	0.064	61.8	0.3	-75.9	0.4

$\sim\alpha$ Maximum deviation of the angle

TABLE II (cont.)

Test Results for Inlet Side Walls at 62 Degrees

y	$\Delta\alpha$	C_{L_∞}	C_{D_∞}	Rey x 10^{-6}	M	V_0	V_3
0.75	139.3	5.98	0.899	1.04	0.175	200.0	313.3
1.00	138.6	5.74	0.682	1.07	0.176	199.1	314.8
2.00	133.0	5.14	0.372	1.10	0.181	205.6	324.5
3.00	133.5	5.07	0.231	1.13	0.182	205.6	332.4
4.00	134.4	5.08	0.206	1.17	0.184	207.3	342.0
5.00	134.4	5.08	0.177	1.14	0.183	207.6	339.7
6.00	134.3	5.08	0.226	1.15	0.180	203.0	334.3
7.00	133.5	5.07	0.247	1.09	0.180	205.3	332.1
8.00	132.1	5.08	0.405	1.12	0.186	210.9	332.4
9.00	138.1	5.55	0.434	1.13	0.182	205.4	329.1
9.25	137.7	5.39	0.416	1.10	0.176	200.4	330.6

TABLE III

Overall Loss Coefficients

Loss Coefficient	Two Dimensional	Secondary	Total
66^{o}			
ζ'	0.065	0.030	0.095
ζ	0.070	0.036	0.106
Y	0.073	0.039	0.112
62^{o}			
ζ'	0.065	0.020	0.085
ζ	0.070	0.025	0.095
Y	0.072	0.025	0.097

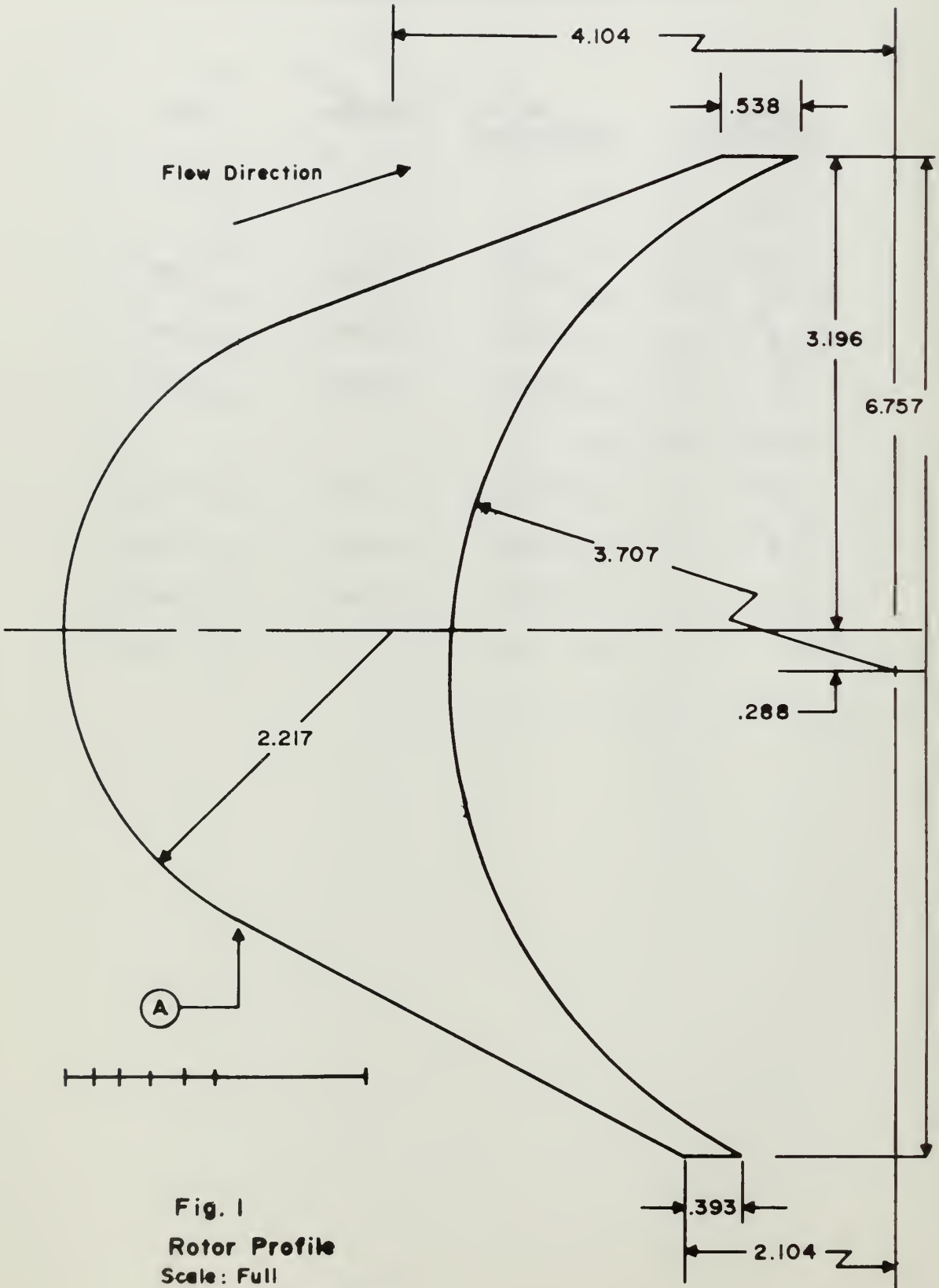

Fig. 1

Rotor Profile

Scale: Full

All dimensions: inches

Fig. 2

Side View of Cascade

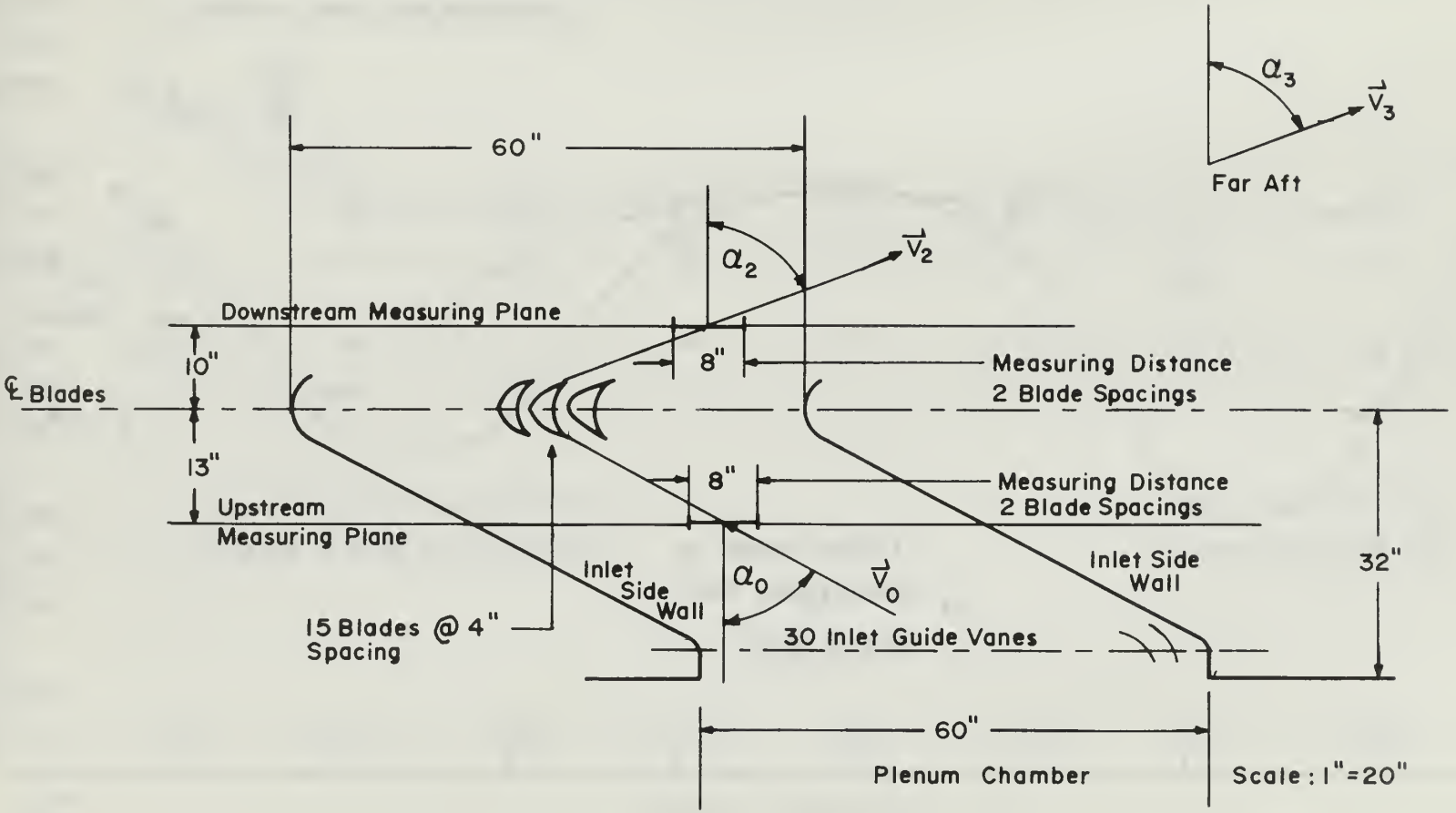

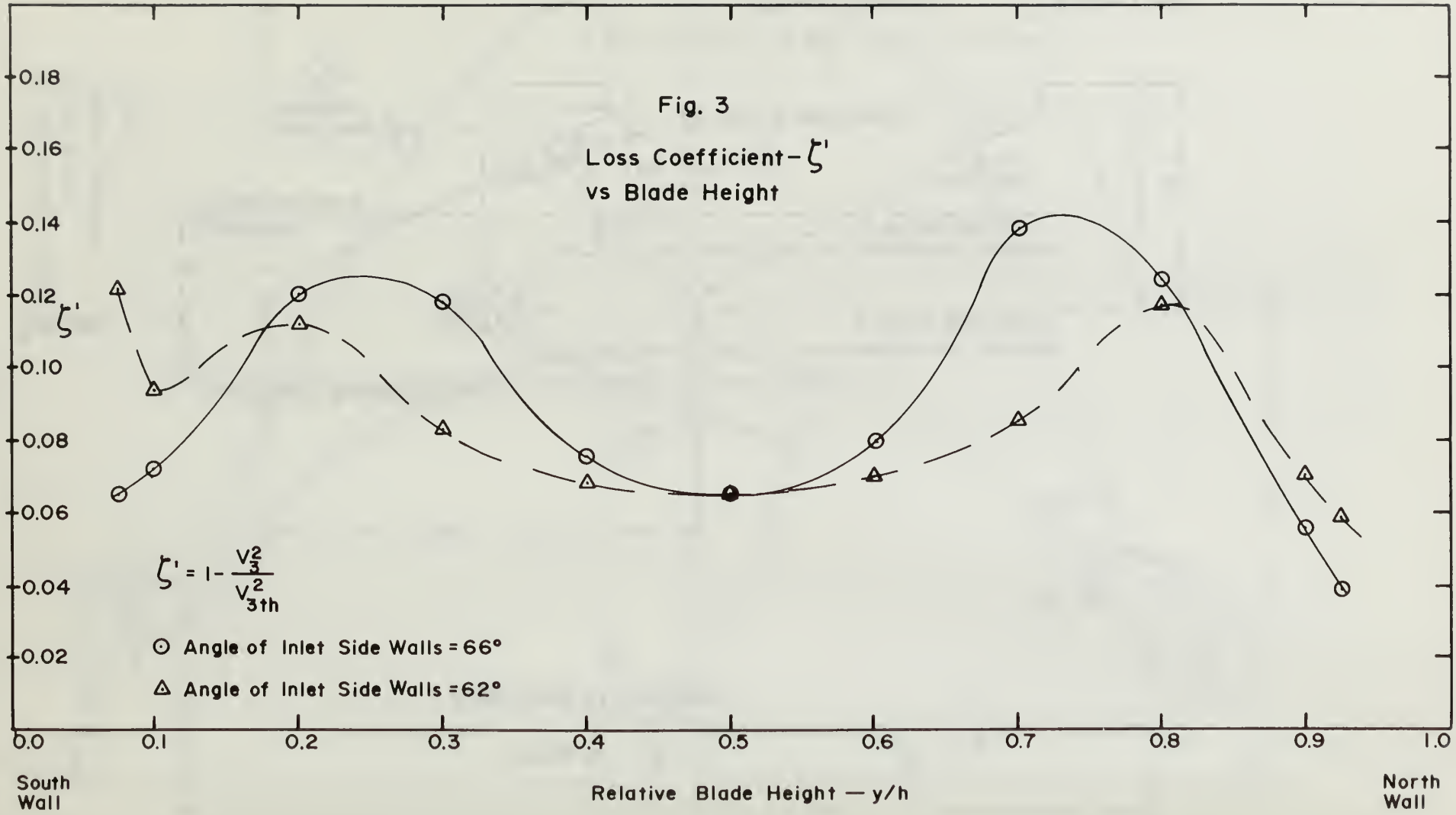
Fig. 3
Loss Coefficient – ζ'
vs Blade Height
0.18
0.16
0.14
0.12
0.10
0.08
0.06
0.04
0.02
ζ'
$\zeta' = 1 - \frac{V_3^2}{V_{3th}^2}$
⊙ Angle of Inlet Side Walls = 66°
△ Angle of Inlet Side Walls = 62°
0.0
0.1
0.2
0.3
0.4
0.5
0.6
0.7
0.8
0.9
1.0
South Wall
Relative Blade Height — y/h
North Wall

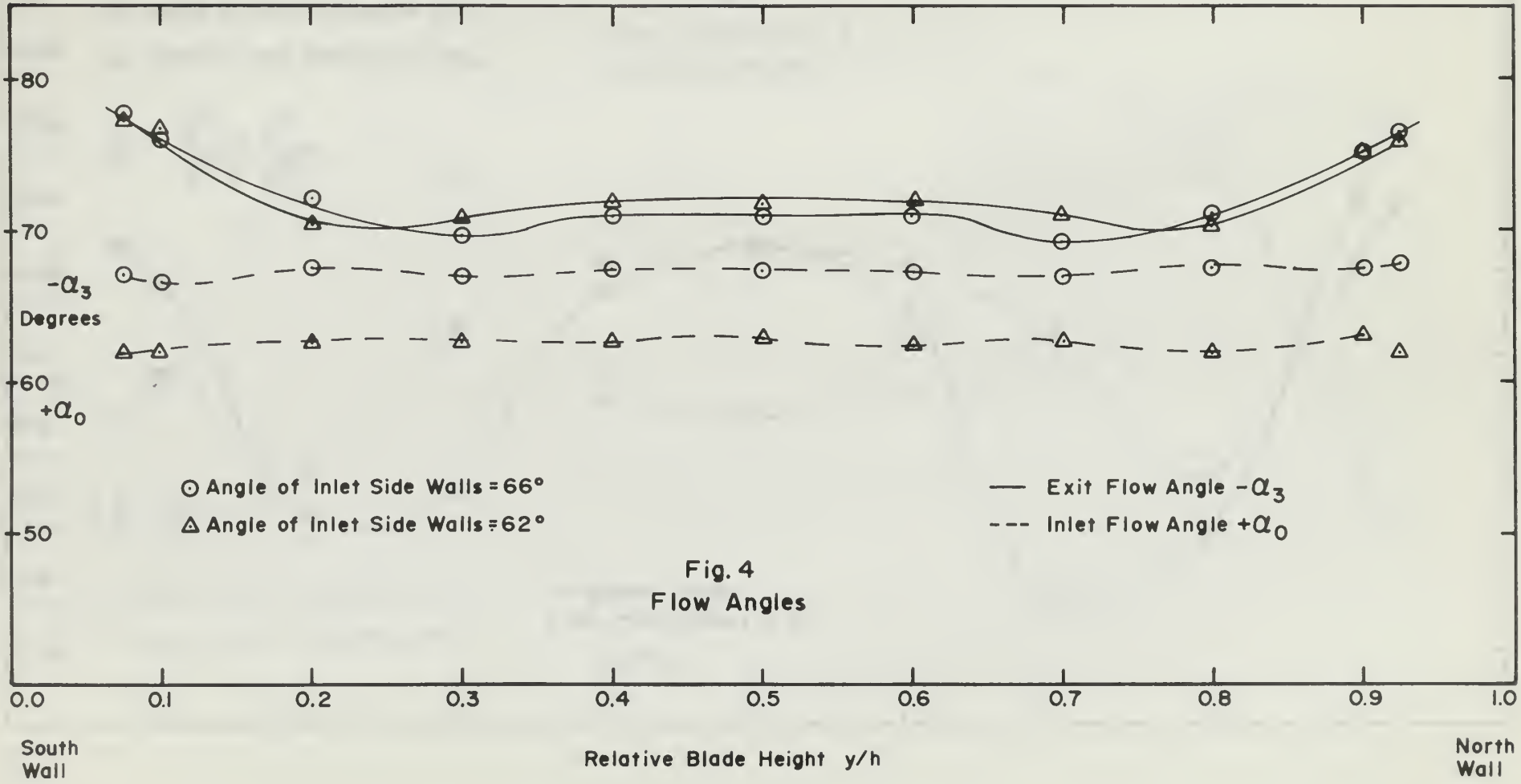

Fig. 4
Flow Angles

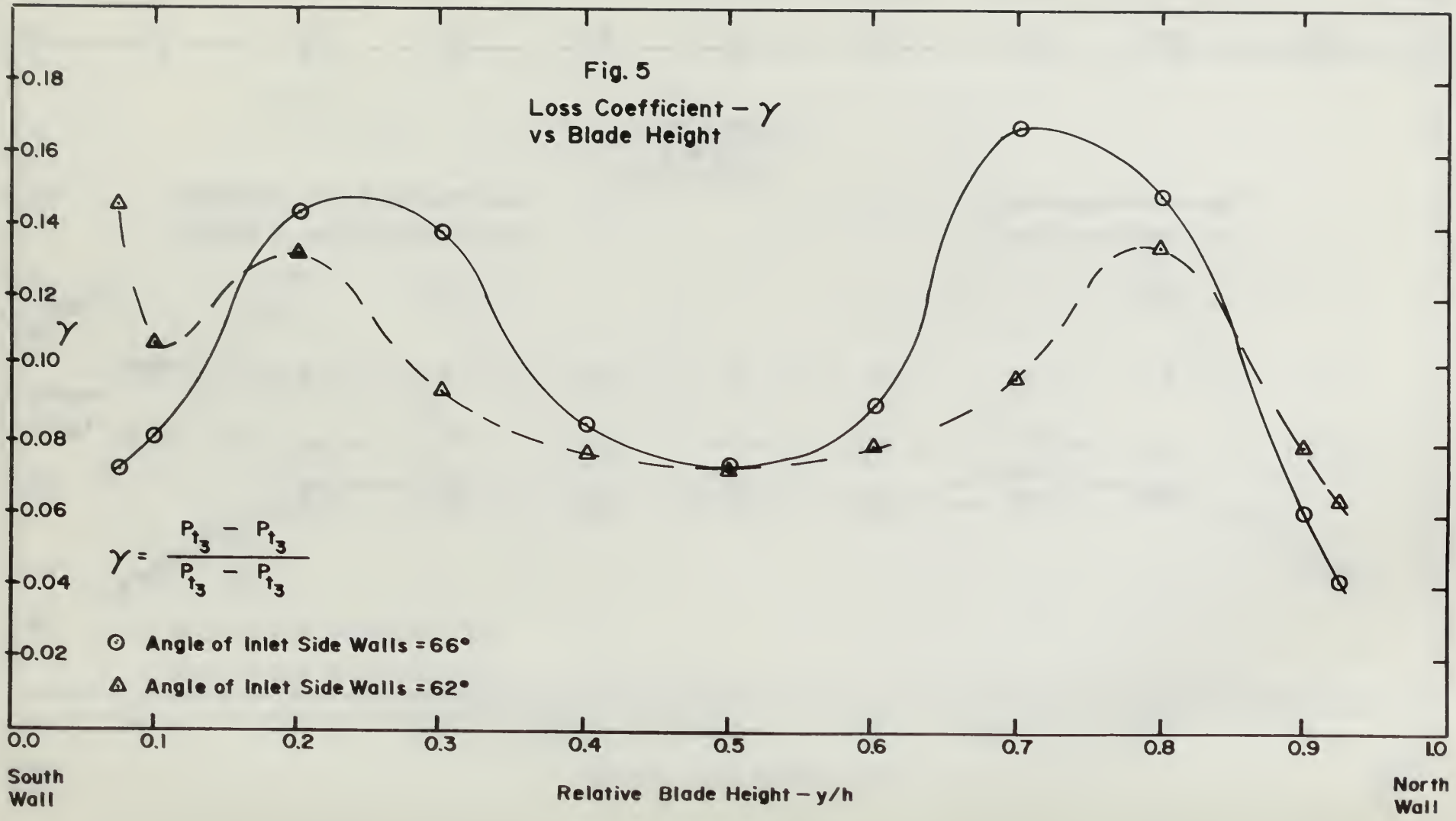
Fig. 5
Loss Coefficient – γ
vs Blade Height
0.18
0.16
0.14
0.12
γ
0.10
0.08
0.06
0.04
0.02
$\gamma = \frac{P_{t_3} - P_{t_3}}{P_{t_3} - P_{t_3}}$
Angle of Inlet Side Walls = 66°
Angle of Inlet Side Walls = 62°
0.0
0.1
0.2
0.3
0.4
0.5
0.6
0.7
0.8
0.9
1.0
South Wall
Relative Blade Height – y/h
North Wall

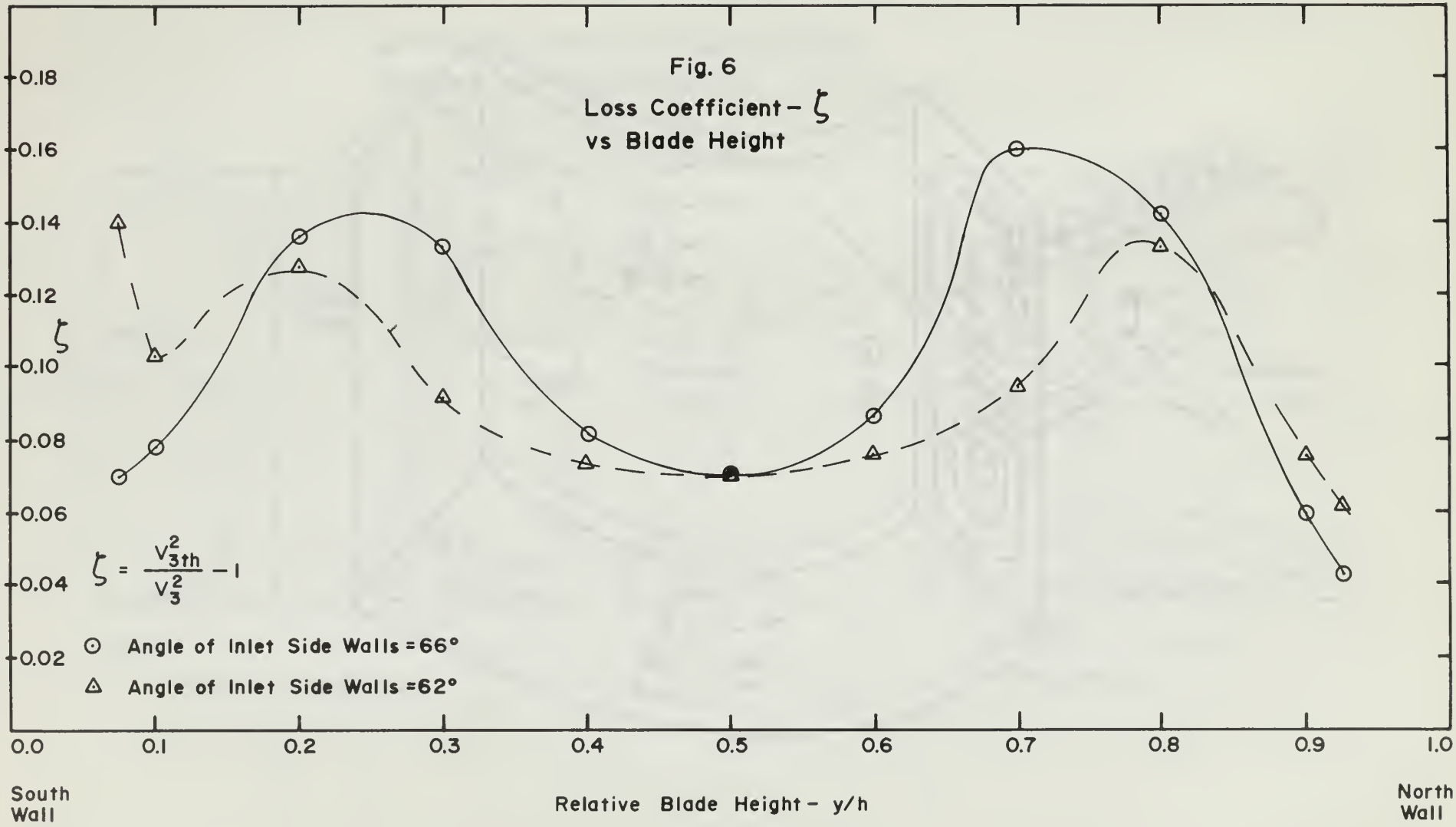
Fig. 6
Loss Coefficient – ζ
vs Blade Height
0.18
0.16
0.14
0.12
0.10
0.08
0.06
0.04
0.02
ζ
$\zeta = \frac{V_{3th}^2}{V_3^2} - 1$
⊙ Angle of Inlet Side Walls = 66°
△ Angle of Inlet Side Walls = 62°
0.0
0.1
0.2
0.3
0.4
0.5
0.6
0.7
0.8
0.9
1.0
South Wall
Relative Blade Height – y/h
North Wall

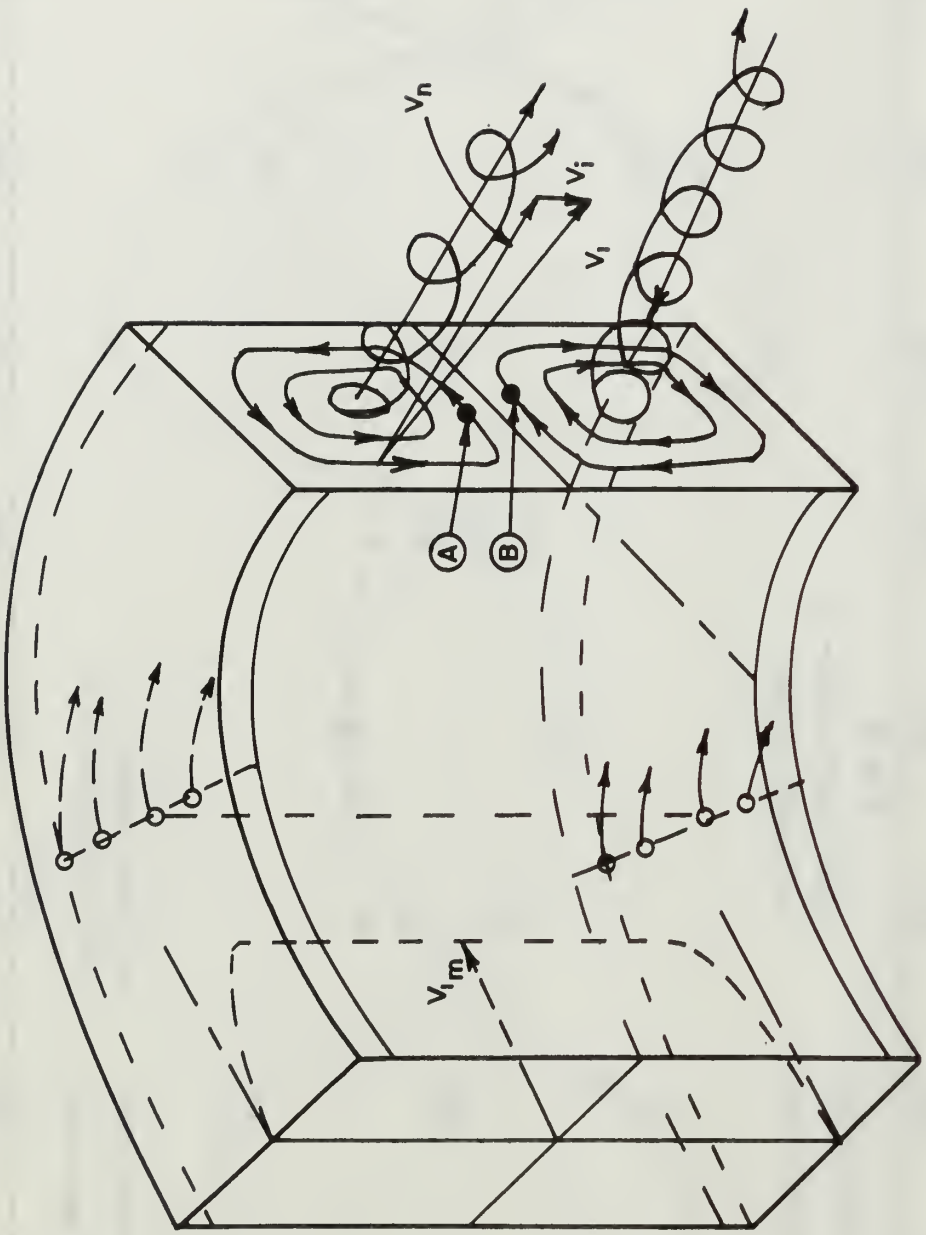

Fig. 7 Secondary Flow in a Bend

Fig. 8

Idealized Three-Dimensional Flow
Through a Row of Blades

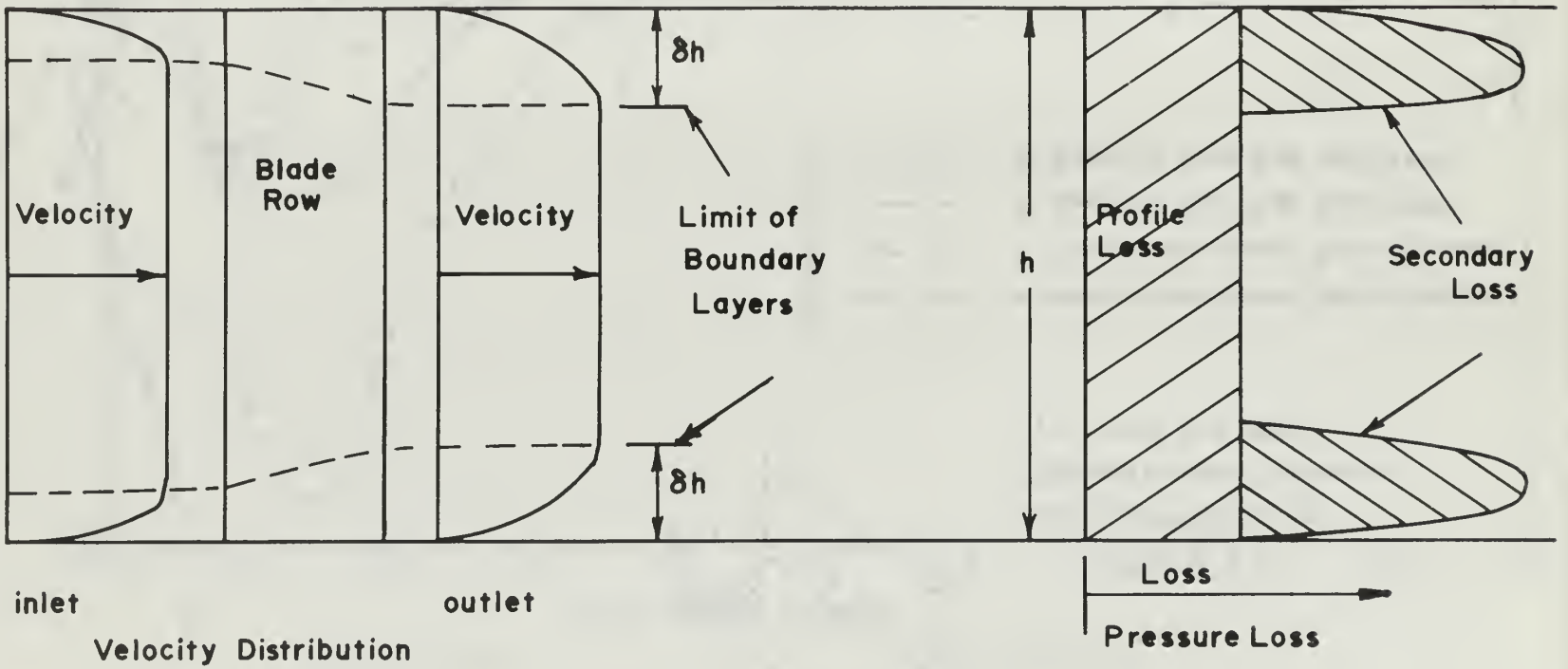

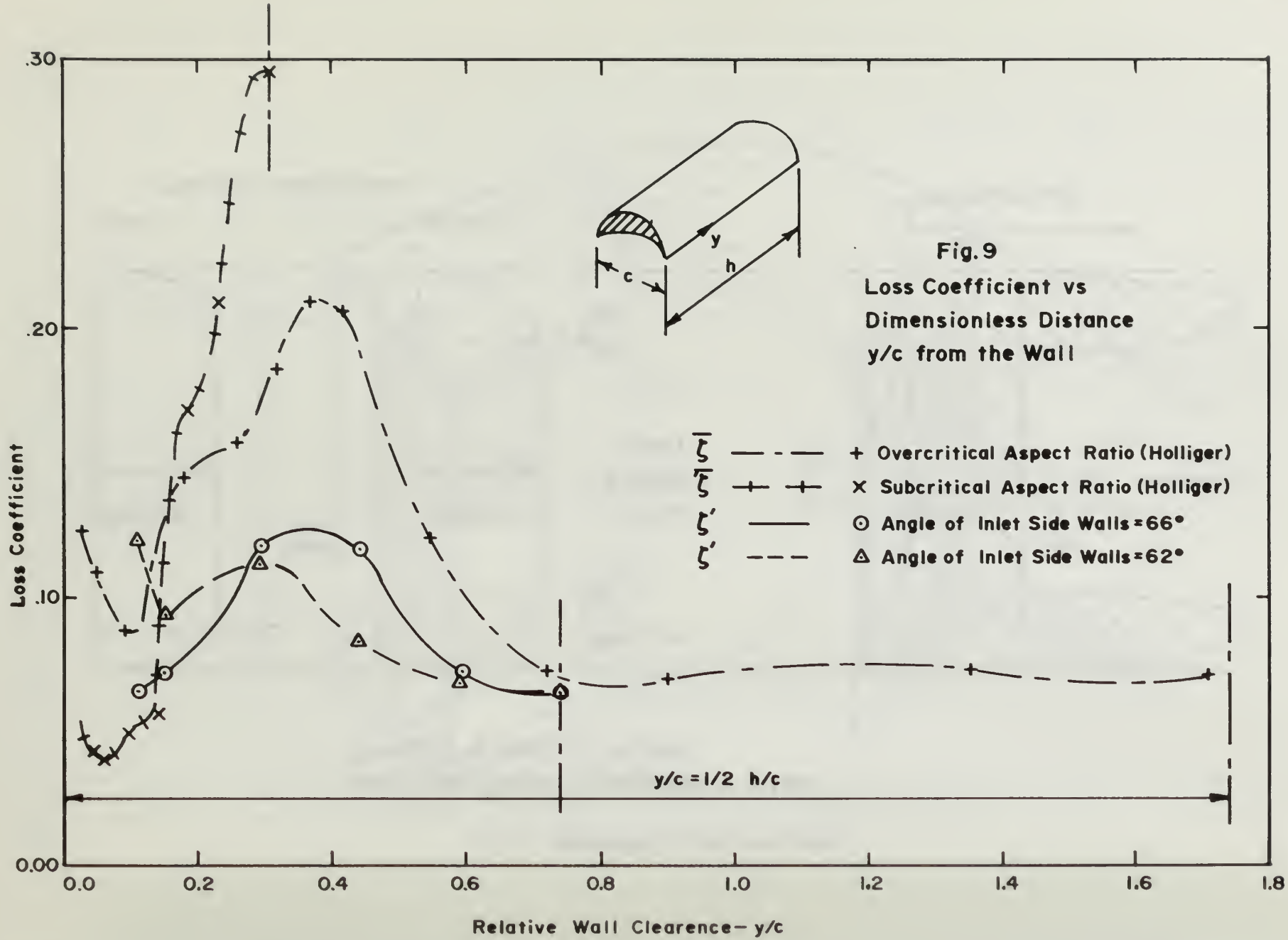

Fig. 9
Loss Coefficient vs
Dimensionless Distance
y/c from the Wall

Fig. 10
Effect of Aspect Raito on
Secondary Flow Loss Pattern
(New)

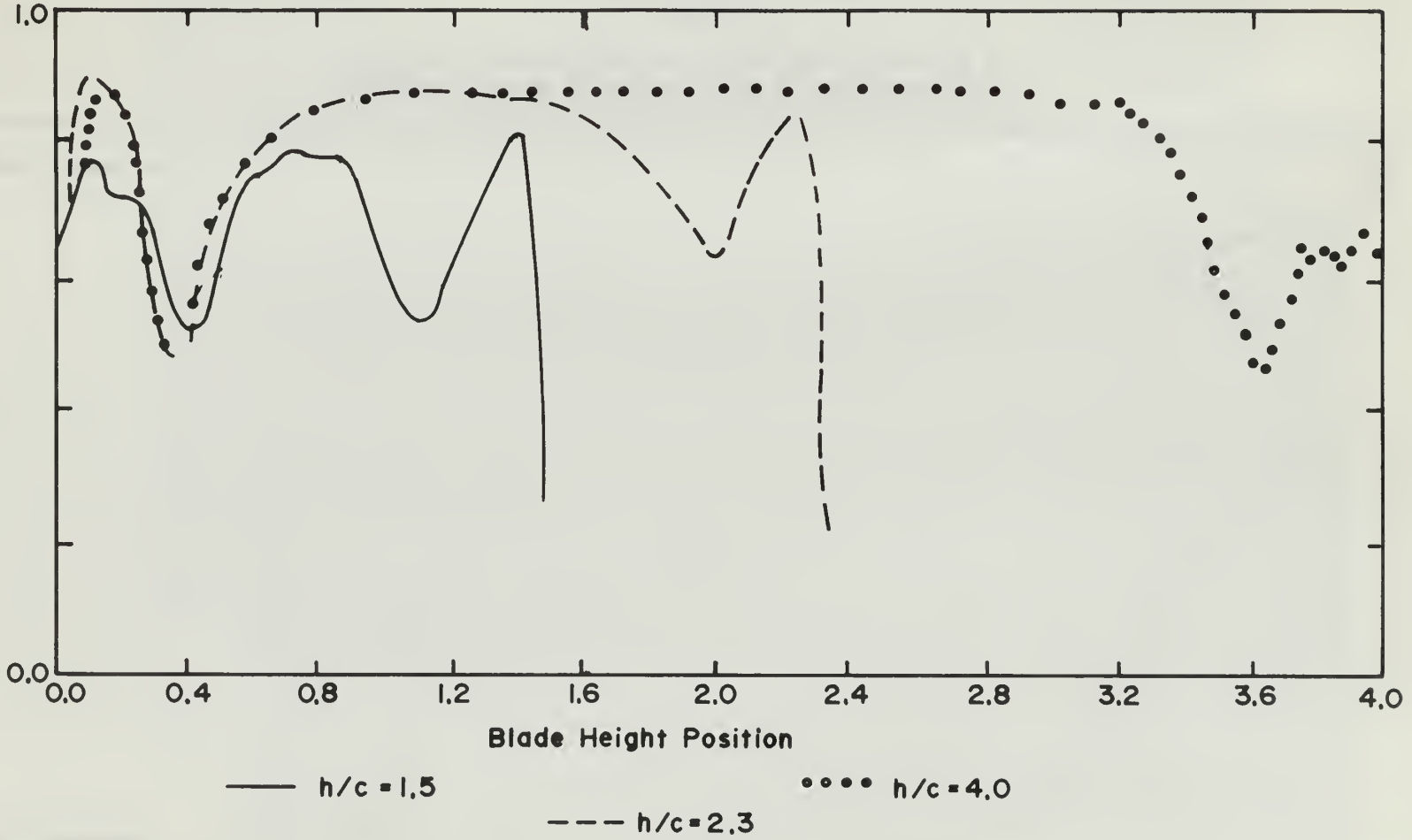

Fig. 12
Typical Distribution of Axial Velocity at Outlet From a Rotor Row (Low Reaction)

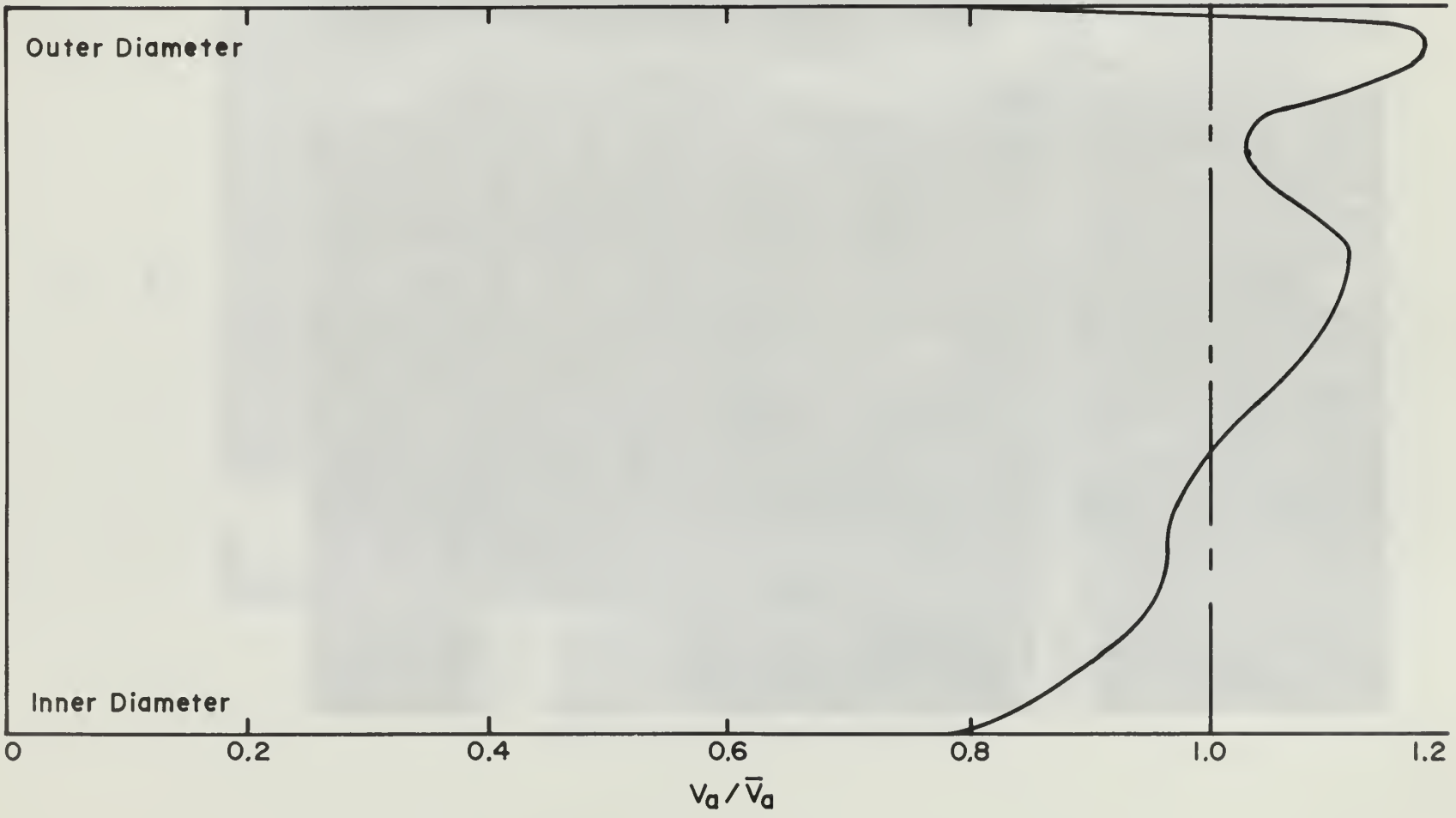

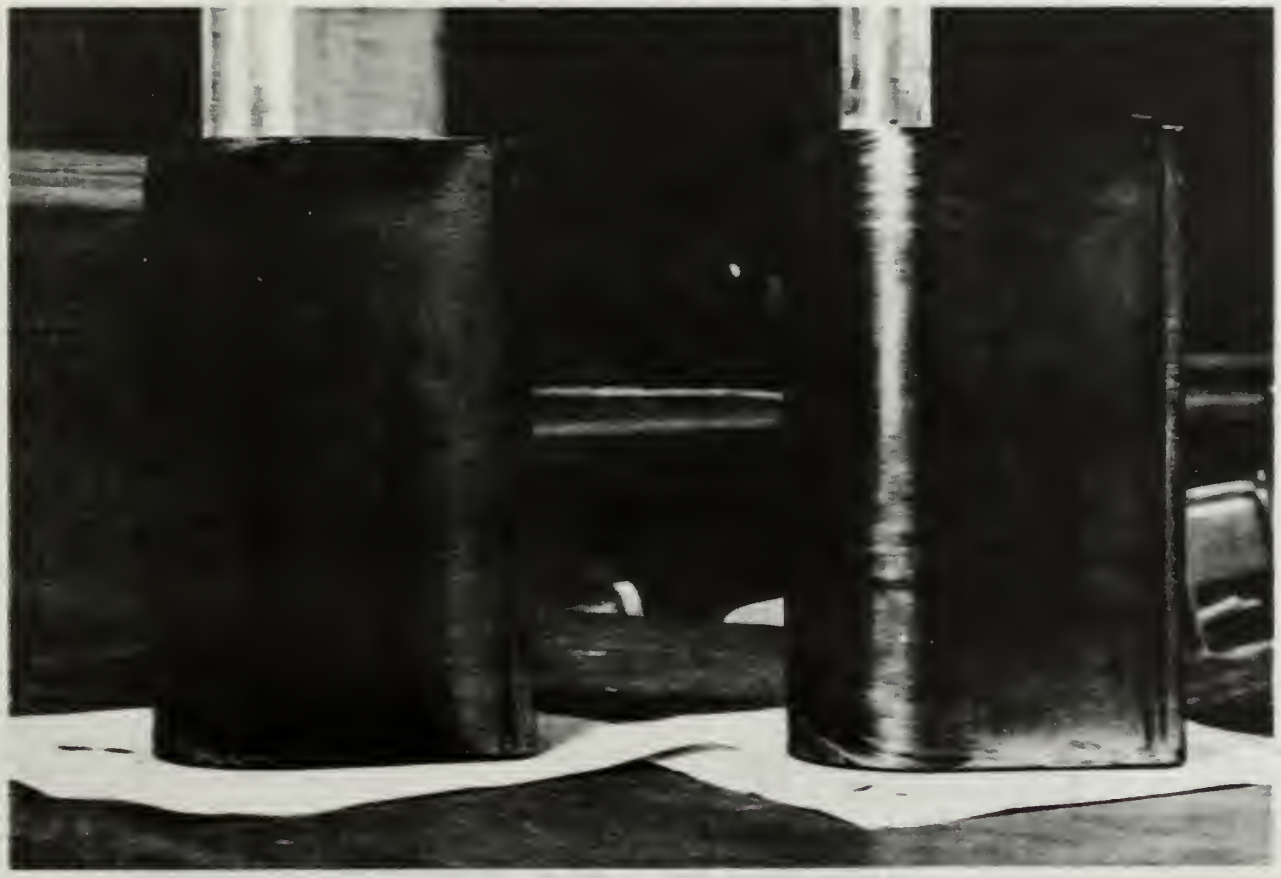

Fig. 13 Leading Edge Boundary Layer
Flow Pattern of the Rotor Blades

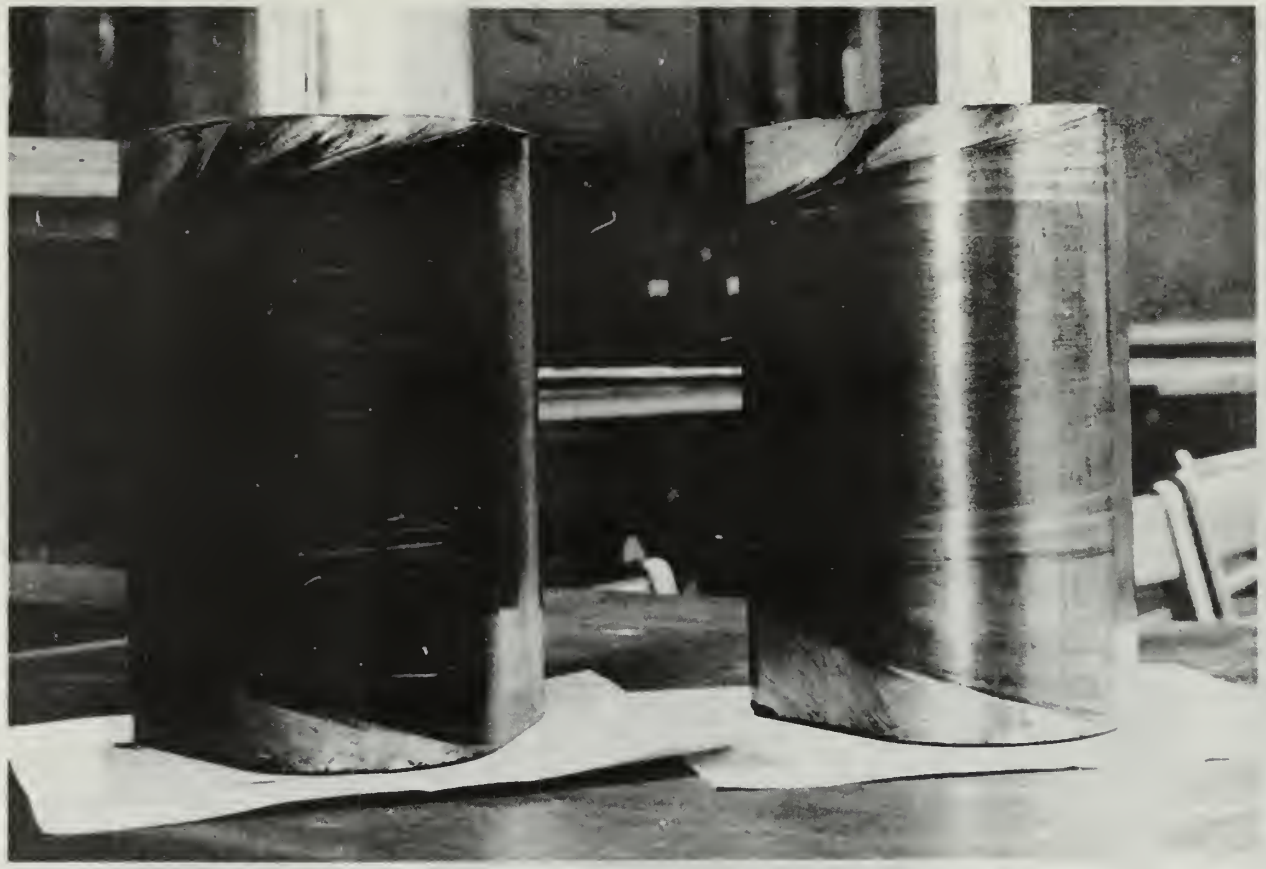

Fig. 14 Mid-Chord Boundary Layer
Flow Pattern of the Rotor Blades

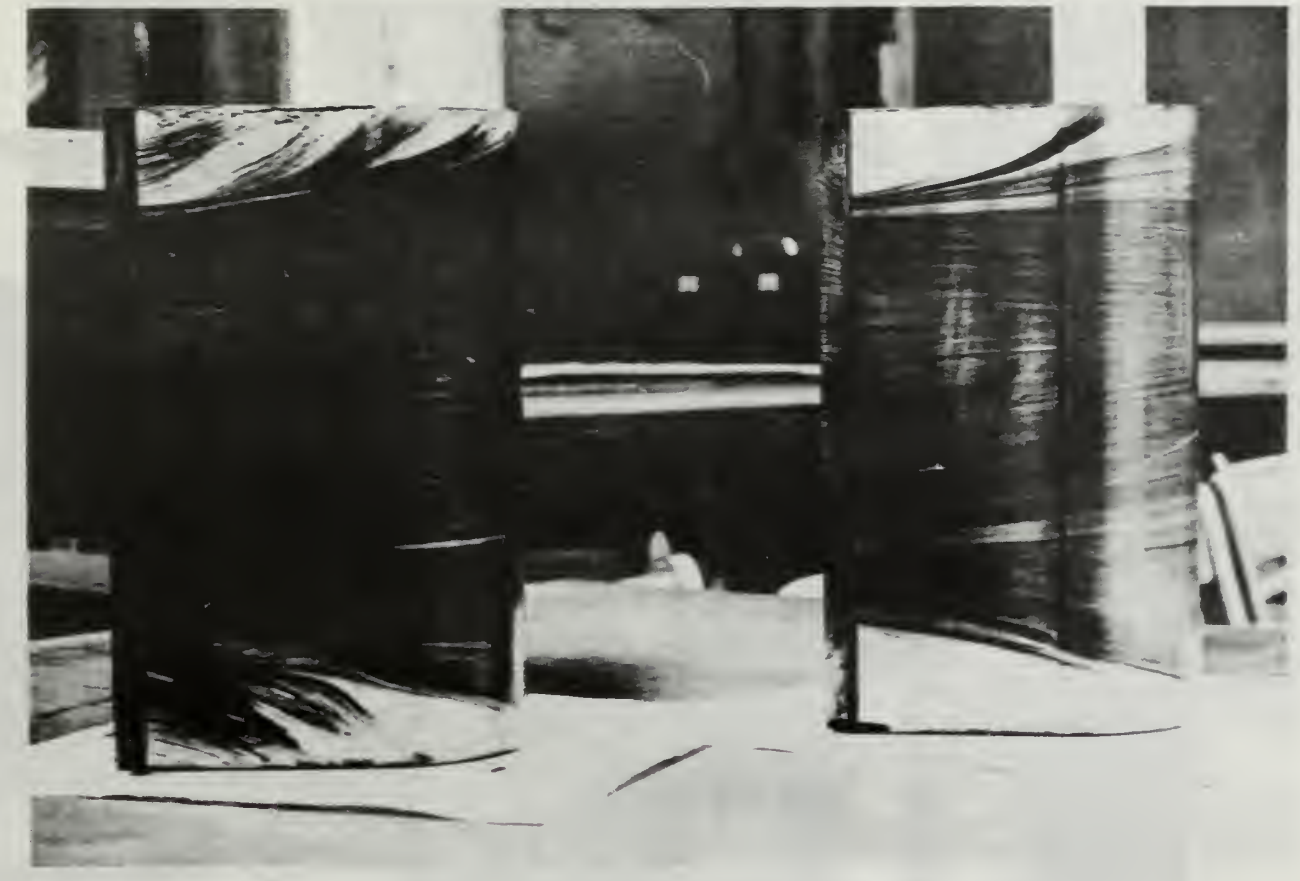

Fig. 15 Trailing Edge Boundary Layer
Flow Pattern of the Rotor Blades

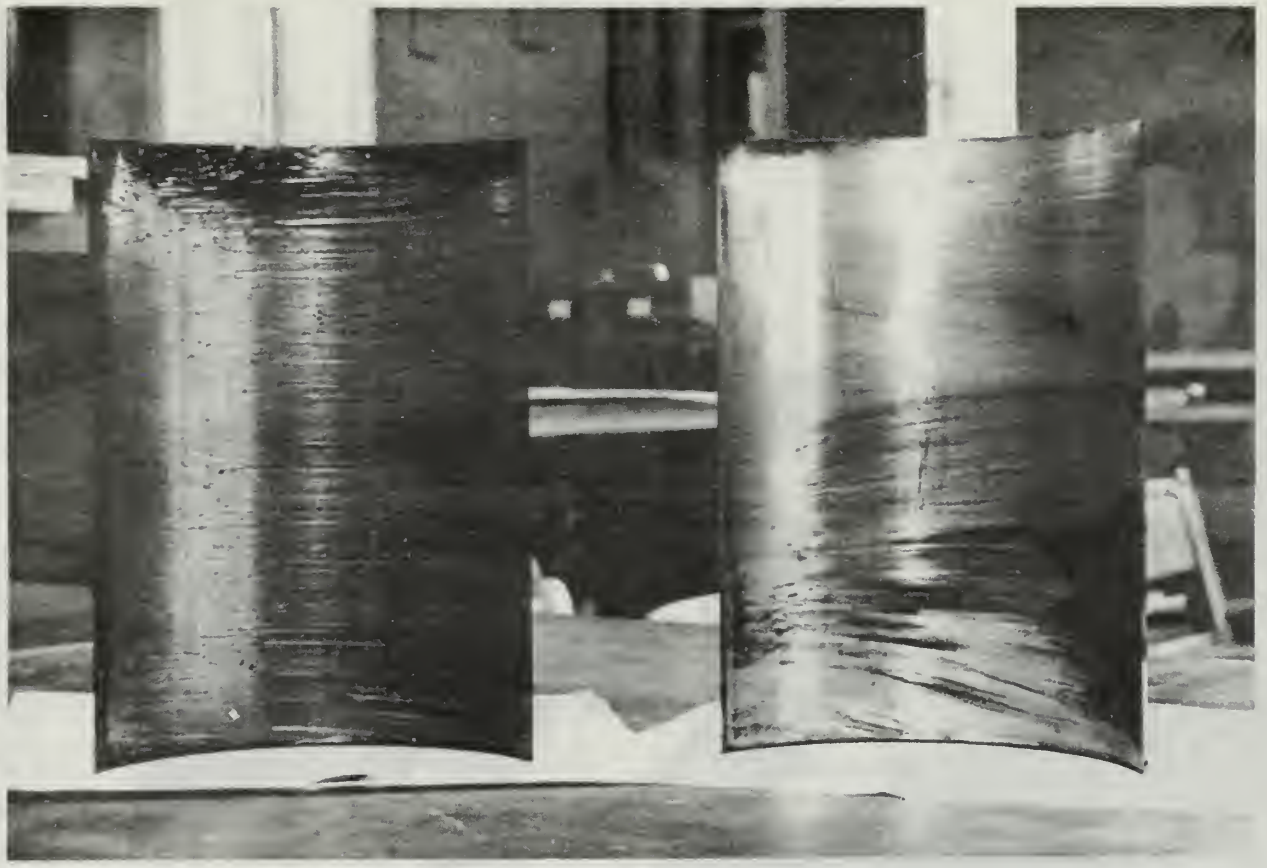

Fig. 16 Concave Side Boundary Layer
Flow Pattern of the Rotor Blades

Fig. 17 Side Wall Boundary
Layer Flow Pattern

BIBLIOGRAPHY

1. Horlock, J. H. Axial Flow Turbines. Butterworth and Co., 1966.

2. Markov, N. M. Calculation of the Aerodynamic Characteristics of Turbine Blading. Associated Technical Services Inc., 1958.

3. Vavra, M. H. Aero-Thermodynamics and Flow in Turbomachines. John Wiley and Sons, 1960.

4. Ainley, D. G. and Mathieson, G. C. R. An Examination of the Flow and Pressure Losses in Blade Rows of Axial-Flow Turbines. Aeronautical Research Council. R and M No. 2891, 1955.

5. Ainley, D. G. and Mathieson, G. C. R. A Method of Performance Estimation for Axial-Flow Turbines. Aeronautical Research Council. R and M No. 2974, 1957.

6. Armstrong, W. D. The Secondary Flow in a Cascade of Turbine Blades. Aeronautical Research Council. R and M No. 2979, 1957.

7. Bartocci, J. E. Cascade Tests of the Blading of a High Deflection, Single Stage, Axial-Flow Impulse Turbine and Comparison of Results with Actual Performance Data. United States Naval Postgraduate School. Thesis, 1966.

8. Bartocci, J. E. An Investigation of the Flow Conditions at the Lower Measuring Plane, and in the Plenum Chamber of the Rectilinear Cascade Test Facility. United States Naval Postgraduate School, Department of Aeronautics. TN No. 66T3, 1966.

9. Eckert, R. H. Performance Analysis and Initial Tests of a Transonic Turbine Test Rig. United States Naval Postgraduate School. Thesis, 1966.

10. Holliger, K. Further Developments of Steam Turbine Blading. Escher Wyss News. v. 33, 1960: 75-81.

11. New, W. R. An Investigation of Energy Losses in Steam-Turbine Elements by Impact Tranverse Static Test With Air at Subacoustic Velocities. Transactions of the ASME. v. 62, August, 1940: 489-500.

12. Rose, C. C. and Guttormson, D. L. Installation and Test of a Rectilinear Cascade. United States Naval Postgraduate School. Thesis, 1964.

13. Vavra, M H. Unpublished Notes.

APPENDIX A

PREDICTION OF EXIT ANGLE

Three formulas were used to estimate the exit angle of the flow of the cascade. The predicted angles were smaller than those experimentally determined but the correlation is quite good. The predicted and experimentally obtained exit flow angles are shown in Table A-I.

1. Markov suggests the use of the following formula to predict the exit angle: [2]

$$\cos \alpha_3 = \frac{a}{s - t_e} \tag{A1}$$

$a = 1.18$ inches $\qquad s = 4.0$ inches

$t_e = 0.538$ inches

From Eq.(A1): $\alpha_3 = 70.0$ degrees.

2. Formula (14) is a curve fit formula based on work done by Vavra. [13]

$$\cos \alpha_3 = \frac{a}{s \cdot K_{te}} \tag{A2}$$

where

$$K_{te} = \frac{\left[1 + 0.01467\left(\frac{t}{s}100\right) - 0.01067\left(\frac{t}{s}100\right)^2\right]}{.888} e^{-0.2375\frac{a}{s}} \tag{A3}$$

$t/s = 0.0525$ $\qquad a/s = 0.295$

$K_{t_e} = 0.820$

From Eq. (A2): $\alpha_3 = 68.9$ degrees.√

3. Ainley and Mathieson use the procedure presented in R. and M. 2974. [5] Formula (A1) is used with the denominator s, rather than

$(s - t_e)$, to obtain $\cos^{-1}(a/s)$. The angle is then obtained by the use of Fig. 5 of R. and M. 2974 which is shown in Fig. A-1.

Eq. (A1) is in agreement with Eckert.[10] From Eq. (A1), $\alpha_3 = 69.5$ degrees.

[10] Eckert, R. H. Performance Analysis and Initial Tests of a Transonic Turbine Test Rig (Thesis, United States Naval Postgraduate School, Monterey, California, 1966) pp. 162.

TABLE A-I

Predicted and Experimentally

Obtained Exit Flow Angles

Predicted	
Markov (Eq. A1)	70.0 degrees
Vavra (Eq. A2)	68.9 "
Ainley and Mathieson (Eq. A1)	69.5 "
Experimental At Centerline	
66^{o} Side Wall Angle	70.8 degrees
62^{o} Side Wall Angle	71.6 "

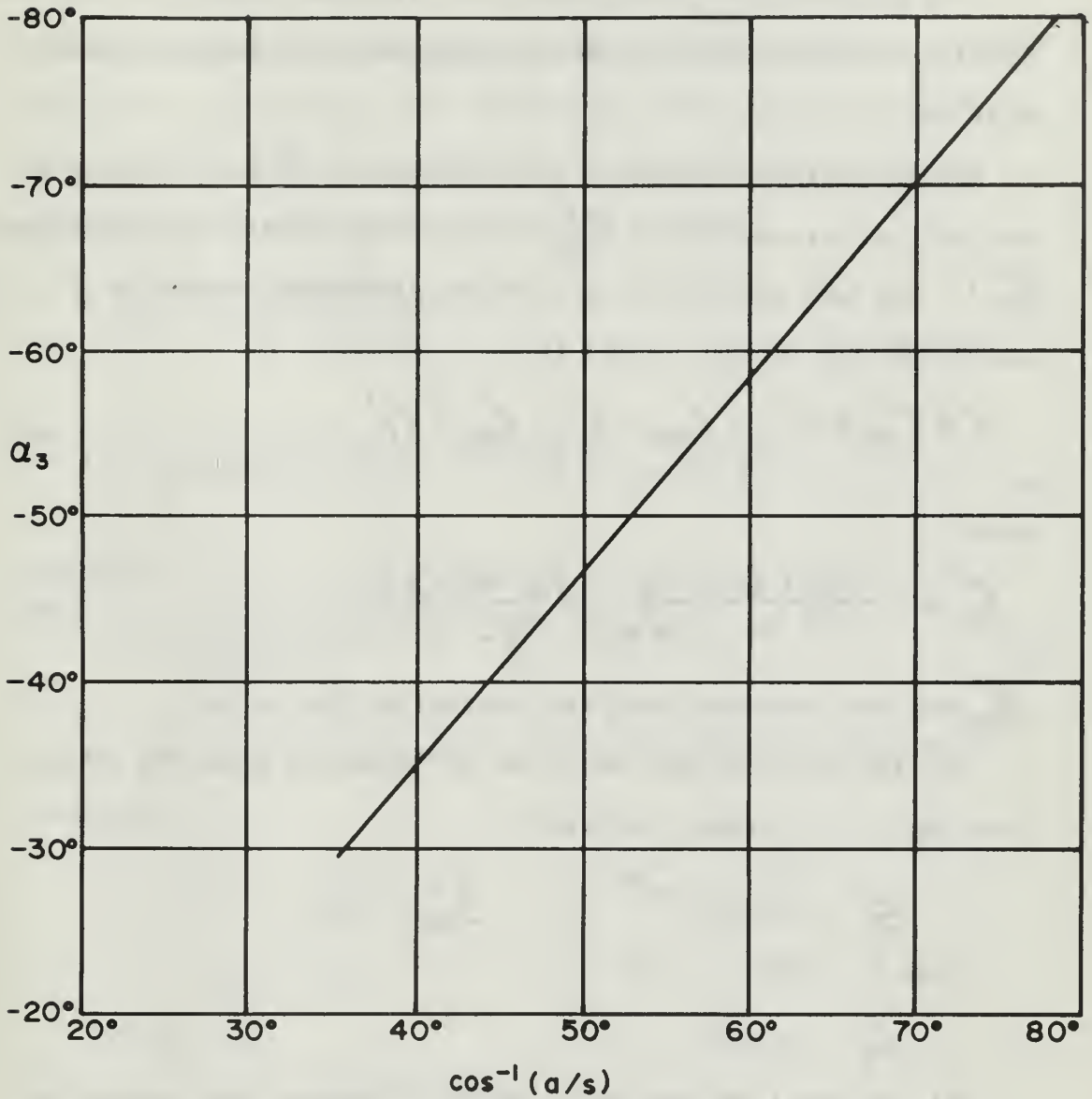

Fig. A-1

Relationship Between Gas Outlet Angles and $\cos^{-1}(a/s)$ for Straight-Backed Blades Operating at Low Mach Numbers (Ainley and Mathieson R and M 2974)

APPENDIX B

PREDICTION OF SECONDARY LOSS COEFFICIENTS

The secondary loss coefficients are calculated using five different formulas. The calculated values are compared to the measured values in Table B-I.

1. Markov develops a secondary loss coefficient ζ_s' that is added to the profile loss coefficient ζ_{2D}' to obtain the overall loss coefficient ζ'.[11] The loss coefficients are defined in the same manner as ζ', in accordance with Eq. (4). There is

$$\zeta' = \zeta_{2D}' + \zeta_s' = \zeta_{2D} + [1 - \zeta_{2D}'] \zeta_\varepsilon' \tag{B1}$$

where

$$\zeta_\varepsilon' = \frac{0.01 (V_0 \sin\alpha_0 - V_3 \sin\alpha_3)}{\cos\alpha_0 \quad V_3 \quad h/c} \tag{B2}$$

ζ_{2D}' has been expressed using the notation of this writer.

a) For the inlet side walls set at 66 degrees where the centerline α_0 = 67.21 degrees there are:

ζ_ε' = 0.0281 $\qquad$ ζ_{2D}' = 0.065

From Eq. (B1)

ζ_s' = 0.0262

b) For the inlet side walls set at 62 degrees where the centerline α_0 = 62.83 degrees there are

ζ_ε' = 0.0220 $\qquad$ ζ_{2D}' = 0.065

[11] Markov, op. cit. pp. 48-50.

From Eq. (B1)

$$\zeta_s' = 0.0206$$

2. Vavra proposes two formulas for predicting the secondary loss coefficient. One uses the lift coefficient, exit angle, and the mean flow angle.[12] This loss coefficient is best compared to the loss Y of Ainley and Mathieson when used with a cascade.

$$C_D = \frac{Y \cos^3 \alpha_\infty}{\sigma \cos^2 \alpha_3} \tag{B3}$$

$$C_D = 0.055 C_{L\infty}^2 \frac{c}{h} = 0.055 C_{L\infty}^2 \sigma \frac{s}{h} \tag{B4}$$

Therefore

$$Y = \frac{0.055 C_{L\infty}^2}{\cos^3 \alpha_\infty} \sigma^2 \frac{s}{h} \cos^2 \alpha_3 \tag{B5}$$

a) For the inlet side walls set at 66 degrees the centerline values are:

$\alpha_3 = -70.8^\circ$ $\qquad$ $\alpha_\infty = -24.67^\circ$

$C_{L_\infty} = 5.85$ $\qquad$ $\sigma = 1.69$

From Eq. (B5)

$$Y = 0.308$$

b) For the inlet side walls set at 62 degrees the centerline values are:

$\alpha_3 = -71.6^\circ$ $\qquad$ $\alpha_\infty = -34.22^\circ$

$C_{L_\infty} = 5.08$

[12] Vavra, op. cit. pp. 336 and 379.

From Eq. (B5)

$$Y = 0.286$$

c) Another formula presented by Vavra uses the velocity ratio $V_{3/V_{3th}}$.[13] The equations have been expressed using the notation of this writer.

$$\zeta' = 1 - \phi^2 \tag{B6}$$

where

$$\phi = 0.99 - \frac{2.28}{10^4}\Delta\alpha - \frac{4.97}{180 - \Delta\alpha} \tag{B7}$$

For $\Delta\alpha = 132^{\circ}$ (design condition): $\phi = .855$

For $\Delta\alpha = 0.0$: $\phi = .928$

The secondary loss can be expressed as the difference between the loss at $\Delta\alpha = 132$ degrees and the two-dimensional loss coefficient.

$$\zeta_s' = \phi_{2D}^2 - \phi^2 = 0.196 \tag{B8}$$

3. Soderberg correlates the loss coefficient to a standard aspect ratio of 3:1 and Reynolds number of 1.0×10^5 which is based on the hydraulic diameter.[14] The expression for the hydraulic diameter is given by Eq. (13). ζ_a is the loss coefficient from Fig. 3.10 of Horlock that is used in Eq. (B9) to predict the loss coefficient at different aspect ratios and Reynolds numbers. Fig. B-1 is a reproduction of Fig. 3.10 from Horlock. Soderberg uses a blade thickness ratio as a parameter in Fig. B-1. The blade thickness ratio for the tested turbine blades is 0.386.

[13] Ibid. pp. 435.

[14] Horlock, op. cit. pp 86-88.

$$\zeta = \left(\frac{10^5}{R_h}\right)^{1/4}\left[(1.0+\zeta_a)(0.975+0.075\,\frac{c}{h})-1.0\right] \qquad \text{(B9)}$$

h = 10.0" s = 4.0"

a) For the inlet side walls set at 66 degrees there are:

$\alpha_3 = 70.8^\circ$ $D_h = 2.32"$

Rey = 1.127×10^6 $R_h = (\frac{D_h}{c})$ Rey = 3.86×10^5

$\Delta\alpha = 138^\circ$

From Fig. B-1

$\zeta_a = 0.14$

Then from Eq. (B9)

$\zeta = 0.12$

b) For the inlet side walls set at 66 degrees there are:

$\alpha_3 = 71.55^\circ$ $D_h = 2.24"$

Rey = 1.136×10^6 $R_h = (\frac{D_h}{c})$ Rey = 3.77×10^5

$\Delta\alpha = 134^\circ$

From Fig. B-1

$\zeta_a = 0.13$

Then from Eq. (B9)

$\zeta = 0.115$

4. Ainley and Mathieson suggest a formula for the secondary loss as a function of the linet and exit areas of the blade row. 4 The secondary loss coefficient Y_s is defined by Eq. (B10).

$$Y_S = \lambda\left(\frac{C_L^2}{s/c}\right)\frac{\cos^2\alpha_3}{\cos^3\alpha_\infty} \qquad \text{(B10)}$$

$$C_L = 2\frac{s}{c}(\tan\alpha_o - \tan\alpha_3)\cos\alpha_\infty \qquad \text{(B11)}$$

$$\lambda = f\left[\frac{(A_2/A_1)^2}{1 + \frac{\text{inner diameter}}{\text{outer diameter}}}\right] \qquad \text{(B12)}$$

λ is obtained from Fig. B-2 which has been reproduced from Ainley and Mathieson.[15]

$$\frac{A_2}{h} = 3.46 \quad \cos 70^\circ = 1.284$$

$$\frac{A_1}{h} = 3.61 \quad \cos 62^\circ = 1.692$$

$$\left(\frac{A_2}{A_1}\right)^2 = 0.57$$

The diameter ratio in the denominator of Eq. (B12) was taken as unity. Then $\lambda = 0.11$ from Fig. B-2.

a) For the inlet side walls set at 66 degrees there are

$\alpha_o = 67.21^\circ$ $\qquad$ $\alpha_\infty = -24.27^\circ$

$\alpha_3 = -70.8$

From Eq. (B10)

$Y_s = 0.144$

b) For the inlet side walls set at 62 degrees there are:

$\alpha_o = 62.83^\circ$ $\qquad$ $\alpha_\infty = -34.22^\circ$

$\alpha_3 = -71.55^\circ$

From Eq. (B10)

$Y_s = 0.13$

[15]Ainley, op. cit. Fig. 17.

TABLE B-I

Comparison of Predicted and

Experimental Loss Coefficients

Formula	Sidewall Angle	Loss Coefficient	Predicted Value	Experimental Value
Markov (B1)	66.0	ζ'_s	0.0262	0.030
	62.0	ζ'_s	0.0206	0.020
Vavra (B5)	66.0	Y	0.308	0.112
	62.0	Y	0.286	0.097
Vavra (B8)	= 132°	ζ'_s	0.196	0.02 to 0.03
Soderberg (B9)	66.0	ζ	0.120	0.106
	62.0	ζ	0.115	0.095
Ainley (B10)	66.0	Y_s	0.144	0.039
	62.0	Y_s	0.130	0.025

Fig. B-1
Soderbergs Loss Coefficient — ζ_a
(Horlock, Axial Flow Turbines)

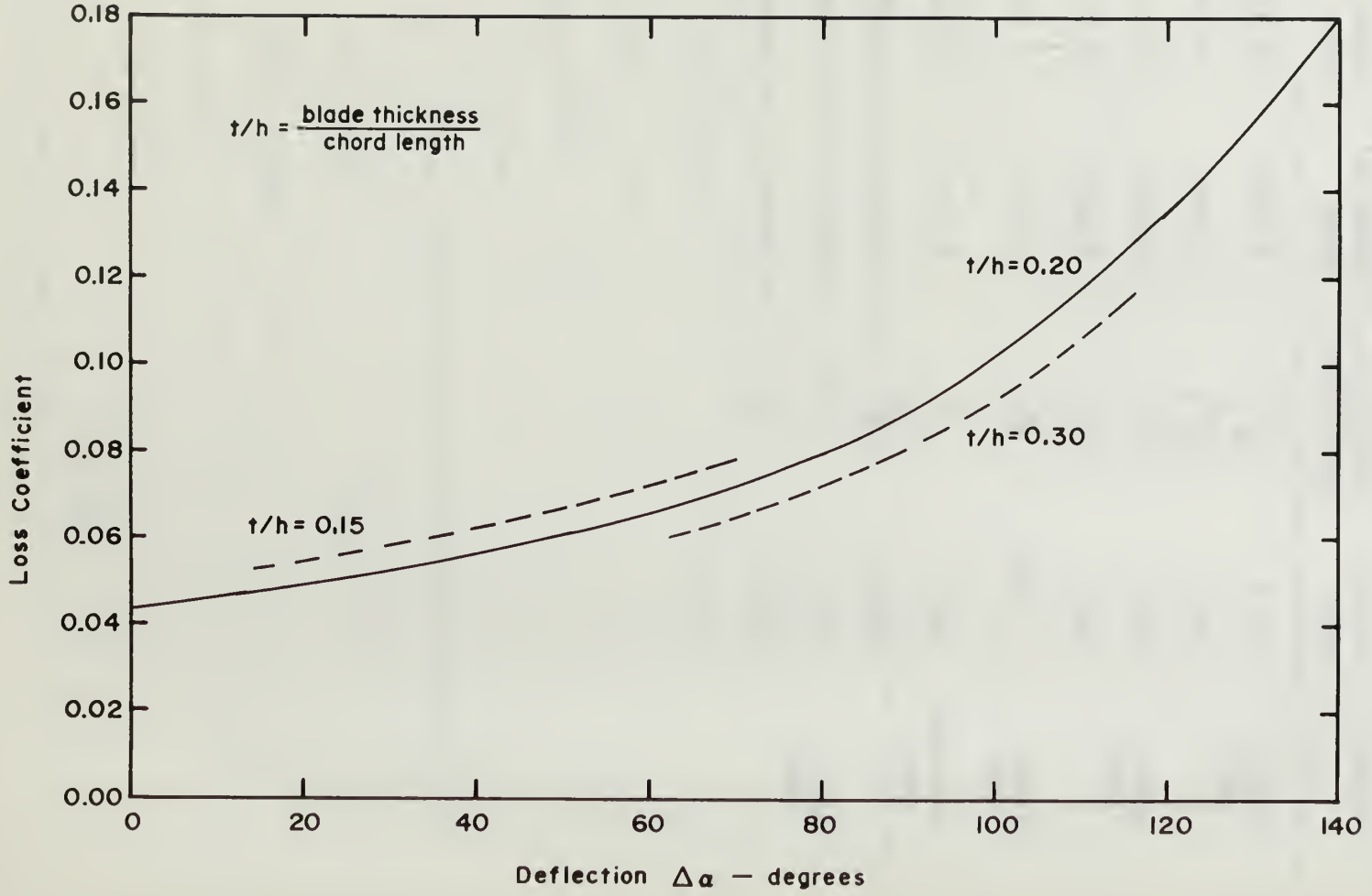

Fig. B-2
Secondary Losses in Turbine Blade Rows
(Ainley and Mathieson R and M 2891)

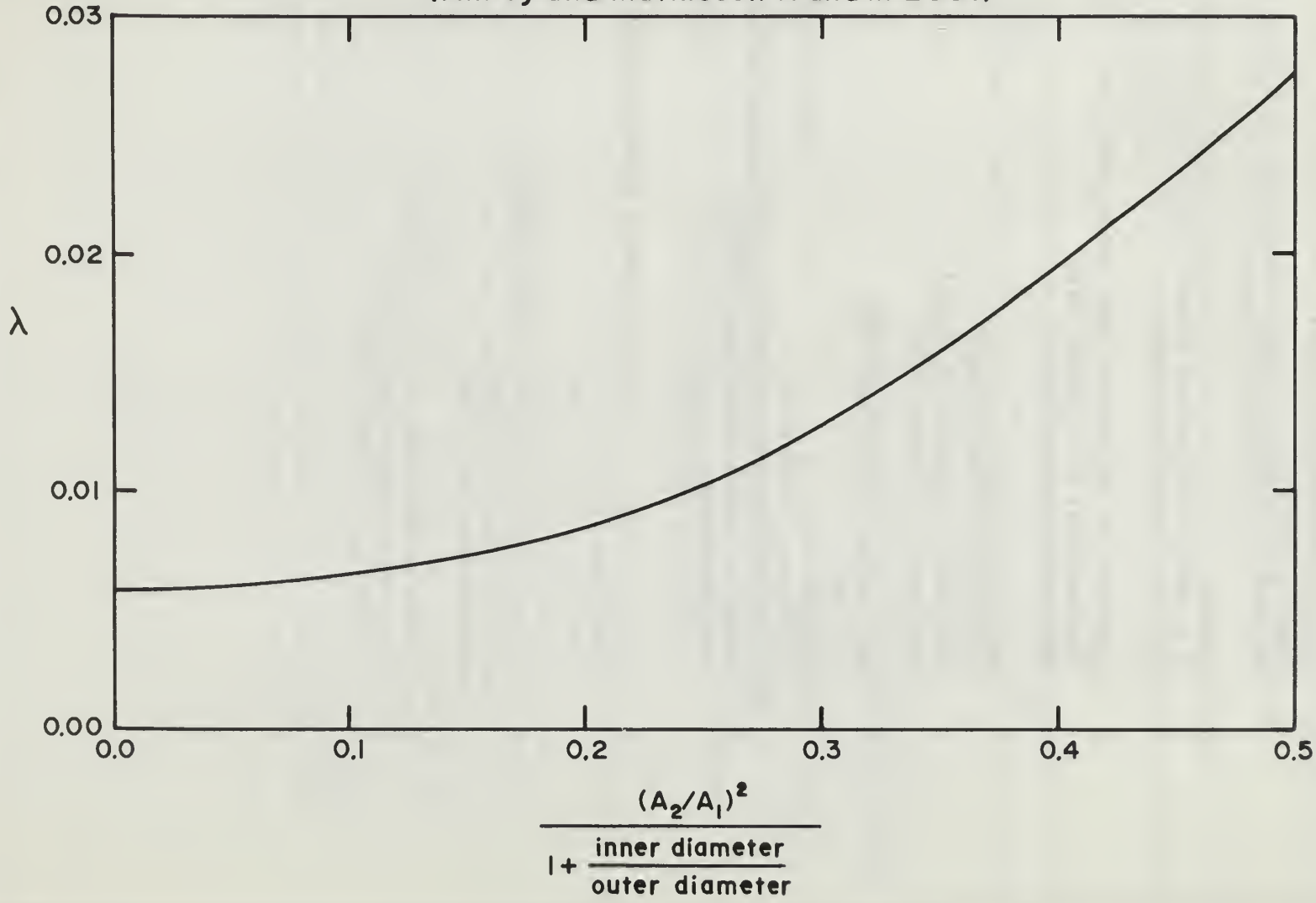

INITIAL DISTRIBUTION LIST

		No. Copies
1.	Defense Documentation Center Cameron Station Alexandria, Virginia 22314	20
2.	Library U.S. Naval Postgraduate School Monterey, California 93940	2
3.	Commandant of the Marine Corps (Code AO3C) Headquarters, U.S. Marine Corps Washington, D. C. 22214	1
4.	Prof. M. H. Vavra Department of Aeronautics U.S. Naval Postgraduate School Monterey, California 93940	3
5.	Capt. Rodney Loren Bown, USMC 3rd MAW MCAS El Toro Santa Ana, California	1
6.	Commander, Naval Air Systems Command Navy Department Washington, D.C. 20360	1
7.	Commander Naval Air Systems Command (BUWEPS/RAPP14) Navy Department Washington, D.C. 20360	1
8.	Office of Naval Research (Power Branch) Department of the Navy Washington, D.C. 20360	1
9.	Chairman, Department of Aeronautics U.S. Naval Postgraduate School Monterey, California 93940	2

DOCUMENT CONTROL DATA - R&D

(Security classification of title, body of abstract and indexing annotation must be entered when the overall report is classified)

1. ORIGINATING ACTIVITY *(Corporate author)*
Naval Postgraduate School
Monterey, California 93940

2a. REPORT SECURITY CLASSIFICATION
UNCLASSIFIED

2b. GROUP

3. REPORT TITLE
AN INVESTIGATION OF THE SECONDARY FLOW PHENOMENA IN A CASCADE OF HIGH-DEFLECTION AXIAL-FLOW IMPULSE TURBINE BLADES

4. DESCRIPTIVE NOTES *(Type of report and inclusive dates)*
Thesis, M.S., December 1966

5. AUTHOR(S) *(Last name, first name, initial)*
BOWN, Rodney Loren

6. REPORT DATE	7a. TOTAL NO. OF PAGES	7b. NO. OF REFS
December 1966	59	13

8a. CONTRACT OR GRANT NO.

b. PROJECT NO.

c.

d.

9a. ORIGINATOR'S REPORT NUMBER(S)

9b. OTHER REPORT NO(S) *(Any other numbers that may be assigned this report)*

10. AVAILABILITY/LIMITATION NOTICES

#1 Memo dtd 12/22/69

Qualified requesters may obtain copies of this report from DDC.
This document has been approved for public release and sale; its distribution is unlimited.

11. SUPPLEMENTARY NOTES

12. SPONSORING MILITARY ACTIVITY

13. ABSTRACT

Cascade tests were performed on models of the rotor blades of a high-deflection, axial-flow impulse turbine to determine the secondary flow losses. The tests were performed at the Rectilinear Cascade Test Facility of the Turbo-Propulsion Laboratories of the Department of Aeronautics, Naval Postgraduate School. The results were compared with the predicted losses from various formulas that have been proposed in the technical literature. The comparison showed that most formulas predict a secondary loss that is about ten times as high as that determined in the present tests. Photographs were obtained of the boundary layer traces by the use of lamp black coating. These photographs show the effects of secondary flows on the performance of a cascade.

DD FORM 1 JAN 64 1473

14. KEY WORDS	LINK A		LINK B		LINK C	
	ROLE	WT	ROLE	WT	ROLE	WT
Turbine Cascade Secondary Flow						

INSTRUCTIONS

1. ORIGINATING ACTIVITY: Enter the name and address of the contractor, subcontractor, grantee, Department of Defense activity or other organization *(corporate author)* issuing the report.

2*a*. REPORT SECURITY CLASSIFICATION: Enter the overall security classification of the report. Indicate whether "Restricted Data" is included. Marking is to be in accordance with appropriate security regulations.

2*b*. GROUP: Automatic downgrading is specified in DoD Directive 5200.10 and Armed Forces Industrial Manual. Enter the group number. Also, when applicable, show that optional markings have been used for Group 3 and Group 4 as authorized.

3. REPORT TITLE: Enter the complete report title in all capital letters. Titles in all cases should be unclassified. If a meaningful title cannot be selected without classification, show title classification in all capitals in parenthesis immediately following the title.

4. DESCRIPTIVE NOTES: If appropriate, enter the type of report, e.g., interim, progress, summary, annual, or final. Give the inclusive dates when a specific reporting period is covered.

5. AUTHOR(S): Enter the name(s) of author(s) as shown on or in the report. Enter last name, first name, middle initial. If military, show rank and branch of service. The name of the principal author is an absolute minimum requirement.

6. REPORT DATE: Enter the date of the report as day, month, year, or month, year. If more than one date appears on the report, use date of publication.

7*a*. TOTAL NUMBER OF PAGES: The total page count should follow normal pagination procedures, i.e., enter the number of pages containing information.

7*b*. NUMBER OF REFERENCES: Enter the total number of references cited in the report.

8*a*. CONTRACT OR GRANT NUMBER: If appropriate, enter the applicable number of the contract or grant under which the report was written.

8*b*, 8*c*, & 8*d*. PROJECT NUMBER: Enter the appropriate military department identification, such as project number, subproject number, system numbers, task number, etc.

9*a*. ORIGINATOR'S REPORT NUMBER(S): Enter the official report number by which the document will be identified and controlled by the originating activity. This number must be unique to this report.

9*b*. OTHER REPORT NUMBER(S): If the report has been assigned any other report numbers *(either by the originator or by the sponsor)*, also enter this number(s).

10. AVAILABILITY/LIMITATION NOTICES: Enter any limitations on further dissemination of the report, other than those imposed by security classification, using standard statements such as:

(1) "Qualified requesters may obtain copies of this report from DDC."

(2) "Foreign announcement and dissemination of this report by DDC is not authorized."

(3) "U. S. Government agencies may obtain copies of this report directly from DDC. Other qualified DDC users shall request through _____."

(4) "U. S. military agencies may obtain copies of this report directly from DDC. Other qualified users shall request through _____."

(5) "All distribution of this report is controlled. Qualified DDC users shall request through _____."

If the report has been furnished to the Office of Technical Services, Department of Commerce, for sale to the public, indicate this fact and enter the price, if known.

11. SUPPLEMENTARY NOTES: Use for additional explanatory notes.

12. SPONSORING MILITARY ACTIVITY: Enter the name of the departmental project office or laboratory sponsoring *(paying for)* the research and development. Include address.

13. ABSTRACT: Enter an abstract giving a brief and factual summary of the document indicative of the report, even though it may also appear elsewhere in the body of the technical report. If additional space is required, a continuation sheet shall be attached.

It is highly desirable that the abstract of classified reports be unclassified. Each paragraph of the abstract shall end with an indication of the military security classification of the information in the paragraph, represented as *(TS)*, *(S)*, *(C)*, *or (U)*.

There is no limitation on the length of the abstract. However, the suggested length is from 150 to 225 words.

14. KEY WORDS: Key words are technically meaningful terms or short phrases that characterize a report and may be used as index entries for cataloging the report. Key words must be selected so that no security classification is required. Identifiers, such as equipment model designation, trade name, military project code name, geographic location, may be used as key words but will be followed by an indication of technical context. The assignment of links, rules, and weights is optional.

DD FORM 1 JAN 64 1473 (BACK)